REPORT DOCUMENTATION PAGE

Form Approved
OMB No. 0704-0188

1. REPORT DATE *(DD-MM-YYYY)*	**2. REPORT TYPE**	**3. DATES COVERED** *(From - To)*
August 2013	Technical Paper	August 2013- September 2013

4. TITLE AND SUBTITLE
A 205 Hour Krypton Propellant Life Test of the SPT-100 Operating at 2 kW

5a. CONTRACT NUMBER
In-House

5b. GRANT NUMBER

5c. PROGRAM ELEMENT NUMBER

6. AUTHOR(S)
Michael Nakles, William Hargus, Jr., Jorge Delgado, and Ronald Corey

5d. PROJECT NUMBER

5e. TASK NUMBER

5f. WORK UNIT NUMBER
Q09W

7. PERFORMING ORGANIZATION NAME(S) AND ADDRESS(ES)

Air Force Research Laboratory (AFMC)
AFRL/RQRS
1 Ara Drive.
Edwards AFB CA 93524-7013

8. PERFORMING ORGANIZATION REPORT NO.

9. SPONSORING / MONITORING AGENCY NAME(S) AND ADDRESS(ES)
Air Force Research Laboratory (AFMC)
AFRL/RQR
5 Pollux Drive
Edwards AFB CA 93524-7048

10. SPONSOR/MONITOR'S ACRONYM(S)

11. SPONSOR/MONITOR'S REPORT NUMBER(S)
AFRL-RQ-ED-TP-2013-223

12. DISTRIBUTION / AVAILABILITY STATEMENT
Distribution A: Approved for Public Release; Distribution Unlimited. PA#13487

13. SUPPLEMENTARY NOTES
Conference paper for the International Electric Propulsion Conference 2013, Washington, D.C., 8 October 2013.

14. ABSTRACT
A life test study was performed on the Russian SPT-100 operating with krypton propellant to obtain channel erosion data. In these experiments, a new flight model SPT-100 was fired with krypton propellant for 205 hours at a power level of 2 kW. This 390 V, 5.1 A operating condition was chosen from a set of operating conditions where krypton performance was characterized in an earlier study.[1] Erosion measurements of the boron nitride channels were taken at 100 hours and 205 hours. A Micro Photonics optical profilometer was used to measure the surface profiles of the ceramic insulators. Cross-section profiles were made in a radially symmetric spoke pattern in 2.5° increments around the thruster face with a lateral resolution of 0.10 mm. These measurements were compared to existing erosion data with xenon.

15. SUBJECT TERMS

16. SECURITY CLASSIFICATION OF:			**17. LIMITATION OF ABSTRACT**	**18. NUMBER OF PAGES**	**19a. NAME OF RESPONSIBLE PERSON**
					William Hargus
a. REPORT	**b. ABSTRACT**	**c. THIS PAGE**	SAR	48	**19b. TELEPHONE NO** *(include area code)*
Unclassified	**Unclassified**	**Unclassified**			661-525-6799

A 205 Hour Krypton Propellant Life Test of the SPT-100 Operating at 2 kW

IEPC-2013-347

Presented at the 33rd International Electric Propulsion Conference, Washington D.C., United States October 6–10, 2013

Michael R. Nakles*
ERC, Inc., Edwards Air Force Base, CA, 93524

William A. Hargus, Jr.†
Air Force Research Laboratory, Edwards Air Force Base, CA 93524

Jorge J. Delgado‡ and Ronald L. Corey§
Space Systems/Loral, Palo Alto, CA 94303

A life test study was performed on the Russian SPT-100 operating with krypton propellant to obtain channel erosion data. In these experiments, a new flight model SPT-100 was fired with krypton propellant for 205 hours at a power level of 2 kW. This 390 V, 5.1 A operating condition was chosen from a set of operating conditions where krypton performance was characterized in an earlier study.[1] Erosion measurements of the boron nitride channels were taken at 100 hours and 205 hours. A Micro Photonics optical profilometer was used to measure the surface profiles of the ceramic insulators. Cross-section profiles were made in a radially symmetric spoke pattern in 2.5° increments around the thruster face with a lateral resolution of 0.10 mm. These measurements were compared to existing erosion data with xenon.

Nomenclature

I_b	integrated thruster beam current
I_d	anode discharge current
I_{sp}	specific impulse
$\dot{m}_a$	anode propellant mass flow rate
$\dot{m}_c$	cathode propellant mass flow rate
$\dot{m}_i$	anode ion mass flow rate
M_0	initial spacecraft mass
M_P	propellant mass for a spacecraft
P	anode power
r	radial distance in thruster coordinate system
V_d	anode discharge voltage
θ	angular position in thruster coordinate system or thruster cant angle
ϕ	azimuth angle within the thruster exit plane

Introduction

For a number of engineering reasons, xenon is the propellant of choice for Hall effect thrusters. These include its high mass (131 amu) and its relatively low ionization potential (12.1 eV). Furthermore, the

*Research Engineer, AFRL/RQRS, 1 Ara Rd. Edwards AFB, CA 93524
†Research Engineer, AFRL/RQRS, 1 Ara Rd. Edwards AFB, CA 93524
‡Senior R&D Engineer, Propulsion Products, 3825 Fabian Way MS G-86
§Mechanical Engineering Specialist, Propulsion Products, 3825 Fabian Way MS G-86

The 33rd International Electric Propulsion Conference, Washington D.C., United States, October 6-10, 2013

inert nature of xenon eliminates the safety concerns that plagued early electrostatic propulsion efforts when mercury and cesium were the standard propellants. Although xenon is a noble gas, it is the most massive, and due to its non-ideal gas behavior, it is possible to pressurize and store at specific densities that exceed unity. As such, it can be stored at higher densities than the common liquid monopropellant hydrazine.[2] While xenon will likely remain the ideal propellant for electrostatic electric propulsion thrusters, the Hall effect thruster community has explored the use alternative propellants for various reasons. Xenon is an expensive resource due to its scarcity and has historically been subject to large price swings due to volatility in the rare gas market.[3] As orbit raising missions of longer duration and larger payloads are proposed for Hall effect thrusters, the mass of required propellant increases. A cheaper propellant could provide significant cost savings for these missions. Also, some missions may benefit from particular thruster performance regimes enabled by the physical properties of certain propellants.

For high thrust to power missions, bismuth has been demonstrated as a viable alternative Hall effect thruster propellant. Bismuth, with its high atomic mass (209 amu) and low ionization potential (7.3 eV) appears to have advantages for missions where high thrust at reduced specific impulse is advantageous, such as orbit raising missions. Bismuth's main drawback is that the metal must be vaporized to be ionized and accelerated within a Hall effect thruster. The requirement for high temperatures (boiling point of 1,837 K) necessitates special engineering considerations compared to the relatively simple gas distribution systems used for xenon. In addition, risk of metal redeposition from the vaporized propellant on solar arrays and sensitive instruments is a large concern that will strongly limit bismuth's appeal to spacecraft designers.

For missions that can benefit from higher specific impulse, krypton may have some benefits. Krypton has a lower atomic mass (83.8 amu) and a higher ionization potential (14.0 eV) than xenon. Like xenon, krypton is a noble gas and could be easily integrated into existing xenon propellant management systems without much modification. The small difference in ionization potential is unlikely to dramatically affect the efficiency of a Hall effect thruster, and the lower mass would produce a 25% increase in specific impulse assuming there were no offsetting losses. The increase in specific impulse could be useful for missions such as GEO communications satellite north-south station keeping. For missions such as orbit raising, increasing the specific impulse will increase trip time because of the corresponding decrease of thrust-to-power ratio. However as solar electric power system specific power increases, increasing the specific impulse of the propulsion system while maintaining a reasonable transfer time may be advantageous.

Krypton is approximately 10 times more common in the atmosphere (and hence in production) than xenon, and when accounting for mass is approximately 6 times less expensive. One disadvantage for krypton is that its tankage fraction appears to be substantially higher than that of xenon due to reduced van der Waals interactions. As such, compressed gas tankage fractions could be as high as 35% compared to 10% for xenon. At least one study has examined this issue and has identified space rated cryo-coolers that could liquefy krypton (120 K boiling point), or for that matter xenon (165 K boiling point), and reduce tankage fractions to less than 2%.[2]

Experimental studies have often shown thrust efficiency with krypton propellant to be inferior to that of xenon.[4,5,6] However, for a 50 kW HET similar thrust efficiency was attained with krypton propellant.[7] Russian studies[5,8,9] have investigated using a mixture of krypton and xenon propellant for SPT thrusters to achieve a performance compromise at a cost cheaper than either pure xenon or pure krypton. Its use has shown promising results on the SPT-100 and SPT-140 thrusters.

Noble gases such as xenon and krypton are byproducts from the process of extracting oxygen from the atmosphere using air separation units (ASU) primarily for use by the steel industry. Air separation units use compression, cooling liquefaction, and fractional distillation to segregate air into its molecular components.[10] However, only large ASUs have the potential to extract rare gases efficiently and not all are configured for this capability.[10] Worldwide, only about 100 ASUs are equipped to extract rare gases from the air.[3] Due to the low natural concentration of rare gases in the atmosphere (87 ppb for Xe and 1.14 ppm for Kr) and the small number of extraction facilities, there is a limited supply of rare gases on the market. The combination of the limited supply and the fluctuating industrial demand for these gases, creates a volatile market. The largest industrial demand for xenon and krypton come from the lighting industry.[3] However, a large spike in the price of xenon (by a factor of 8 to 10) occurred in the years between 2005 and 2008 when industrial demand soared due to the manufacturers of plasma display panel TVs and electronic chips.[3] Another xenon price jump within the next few years is predicted by at least one analyst from xenon's possible application as an anesthetic in Europe.[3] The historical price swings and the uncertainty in future pricing have motivated the electric propulsion community to explore the use of krypton as a potential substitute for xenon in existing

propulsion devices to save money at the expense of reduced efficiency.

Despite krypton's inherently lower performance, it could conceivably fulfill the propulsion requirements of certain missions. This scenario would typically require thruster operation at a higher power and/or with a longer cumulative firing time. This required increase in energy-throughput over the course of the mission would naturally cause concern about the life expectancy of the thruster, which is limited by the erosion of the channel walls and the center magnetic core from sputtering induced by energetic ions. Reliable life time predictions require erosion measurements from ground testing. Unfortunately, little Hall thruster erosion data exist for krypton propellant.

A multi-part study was performed at the Air Force Research Laboratory (AFRL) to characterize the differences between xenon and krypton performance,[1] plume characteristics,[11] and insulator erosion for a Hall effect thruster with extensive flight heritage. The SPT-100 thruster was chosen for this study because it is among the most well-established Hall effect thrusters in the space propulsion industry. SPT design heritage dates back to the 1960s and 70s in the former U.S.S.R. After the break up of the Soviet Union, the Ballistic Missile Defense Organization (BMDO) led efforts to transfer SPT technology to the United States so that western spacecraft could benefit from their attractive combination of thrust and efficiency.[12] The SPT-100 thruster, designed and built by Fakel, was extensively tested for lifetime[12] and performance[12,13] by NASA in the early 1990's. In 1991, Space Systems/Loral (SS/L) partnered with Fakel to flight qualify the SPT-100 and a corresponding power processing unit (PPU) for U.S. flight standards. To date, SS/L has launched seven spacecraft with SPT-100 propulsion subsystems and has eleven more spacecraft under construction. This SPT subsystem now has more than thirteen years of cumulative on-orbit experience with a single thruster accumulating over 6 years of near-daily operation.[14] This paper will present the results from a short (205 h) life test of an SPT-100 operating with krypton gas at a power level of 2 kW where insulator erosion was quantified at the midpoint and the end of the test.

Experimental Apparatus and Techniques

Test Facility

The life test performed in this study utilized Chamber 1 at the Air Force Research Laboratory at Edwards Air Force Base. Chamber 1 is a cylindrical non-magnetic stainless steel vacuum chamber 2.4 m in diameter and 4.1 m in length. Pumping is provided by two liquid nitrogen baffled (70 K), 1.2 m flanged gaseous helium two stage cryogenic (15 K) vacuum pumps. Chamber pressure is monitored with a hot filament ionization gauge. Background pressure for the selected krypton thruster operating condition was measured to be 2.3×10^{-5} Torr (at 4.50 mg/s propellant flow rate) with a gas correction factor[15] applied.

The interior of the chamber is covered with nuclear grade, low sulfur, flexible graphite 1.8 mm thick. Both chamber ends contain louvered beam dumps manufactured in-house using 13 mm thick, 15 cm wide graphite panels to reduce redeposition of sputtered materials on the thruster during extended firings. The chamber floor is protected using a carbon-carbon woven blanket that allows for ease of placement and removal.

Hall Effect Thruster

A flight model SPT-100 Hall effect thruster was used in this study. The axisymmetric thruster is equipped with two lanthanum hexaboride (LaB_6) cathodes (only one was used during these tests). This thruster has a conventional five magnetic core (one inner, four outer) magnetic circuit. Discharge current is routed through the magnetic circuit and thus no extra power source for the magnets is required. The acceleration channel of the thruster has a 100 mm outer diameter, a 69 mm inner diameter, and a channel depth of 25 mm. For its nominal xenon operating condition, the thruster has been characterized to have a thrust of 83 mN with a specific impulse of 1,600 s, yielding an anode efficiency near 50%.[12]

In an earlier study[1] at AFRL, the performance of the SPT-100 operating on krypton was characterized using an inverted pendulum thrust stand over a wide range of thruster operating conditions spanning a power range of 800 W to 3.9 kW. Anode potential and mass flow rate were varied in increments of 10% of their nominal values. The mass flow rate that produced the nominal anode current of 4.50 A was considered the nominal flow rate for krypton. This study also included a smaller set of xenon cases for comparison. The performance characteristics measured are shown in Figs. 2 and 3. Figure 18 shows a simple mission analysis to characterize the requirements of propellant mass and total firing time for two SPT-100s used for North-South Station Keeping (NSSK) on a typical geosynchronous communications satellite for the operating

The 33rd International Electric Propulsion Conference, Washington D.C., United States, October 6-10, 2013

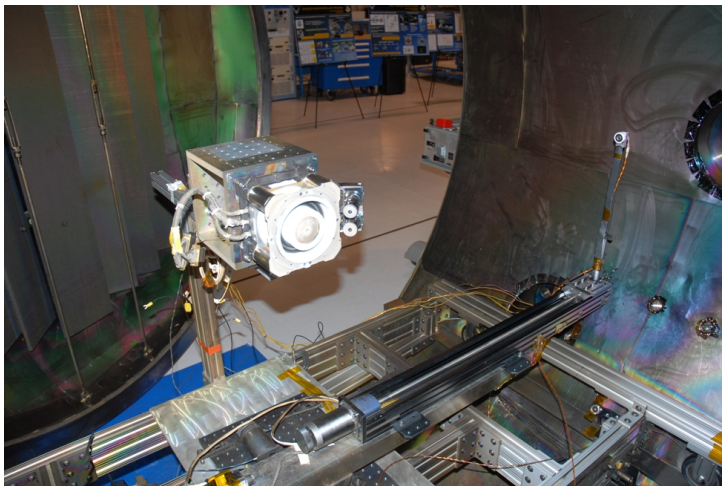

(a) The SPT-100 installed in Chamber 1 before the start of the life test. The Faraday probe was installed to make sweeps at $r = 100$ cm throughout the test.

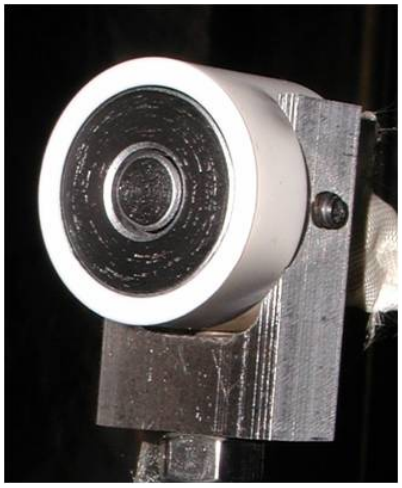

(b) A close-up photo of the Faraday probe. The collector was 8.3 mm in diameter and the guard ring was 22.5 mm in outer diameter.

Figure 1. The Chamber 1 test facility and Faraday probe used for the life test.

conditions where performance was tested. The mission analysis is explained in the appendix.

The criteria in choosing an operating condition for this life test were good performance (relative to the other tested krypton cases), good mission characteristics in the context of the NSSK mission analysis, and a reasonable power level considering the thruster was designed for 1.35 kW. The 390 V, 4.50 mg/s operating condition was selected to meet these guidelines. The higher than nominal discharge potential was chosen to achieve good thruster efficiency. Figure 3(c) shows that the trend of improving thruster efficiency with increasing discharge potential occurs at higher discharge potential values compared to xenon. A mass flow rate producing an anode current about 10% greater than the nominal xenon condition was chosen to acheive a thrust level similar to the nominal xenon operating condition. Figure 2(c) shows an approximately linear increase in thrust as mass flow rate is increased. For the NSSK mission, the required total mass of propellant would be 199 kg with a cummulative firing time of 5,860 h for each thruster. In comparison, the nominal xenon condition would require 246 kg of propellant and a firing time of 6,160 h. In this propellant substitution scenario, 47 kg of propellant mass would be saved with a similar firing time requirement. However, an extra 630 W of power would be necessary. Other high discharge potential operating conditions with lower flow rates requiring more firing time and less power were also feasible choices.

One of the major issues with using this and other krypton operating conditions is determining if the thruster insulators would survive the erosion process over the life of the mission. As seen in Fig. 18, krypton propellant requires higher operating powers and/or longer firing times to impart the mission required ΔV. Encouraging experimental data from one study[16] shows that boron nitride based ceramics have an approximately 30-50% lower erosion rate when bombarded with krypton ions compared to xenon at a given ion energy. For the nominal xenon condition (1.35 kW), tests have validated the SPT-100 life time as exceeding 2.71 million N-s (equivalent to approximately 9,000 hours of operational time).[17,14] The goal of this study was to examine the intial erosion rate of insulators using krypton propellant and compare the results with data from a xenon life test.

Table 1 lists the specifications of the krypton life test operating condition during performance testing and the life test. (Note: The performance testing and life testing were performed using different thrusters.) During the life test, the anode current was 2% higher than its measured value from the performance testing. In both peformance and life tests, the thruster and cathode were powered with commercial off-the-shelf Sorenson power supplies instead of the PPU used on-orbit. A computer data acquisition system recorded the potential and current outputs of the power supplies used in the thruster operation at a rate of 2 Hz during this study. For propellant flow, digital mass flow controllers from Aera dispersed krypton gas to the anode and cathode taking the place of the xenon flow control system (XFC) used on-orbit.

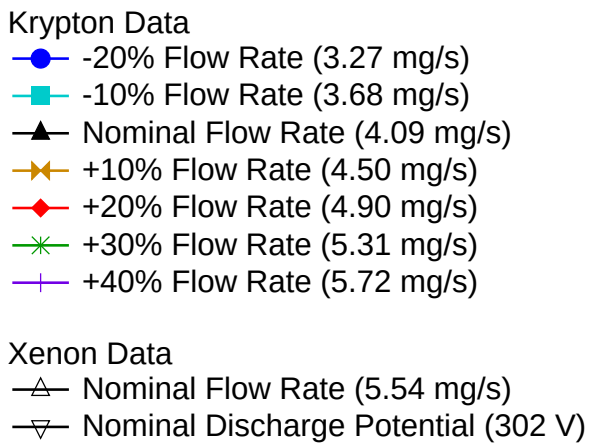

(a) Legend for performance plots.

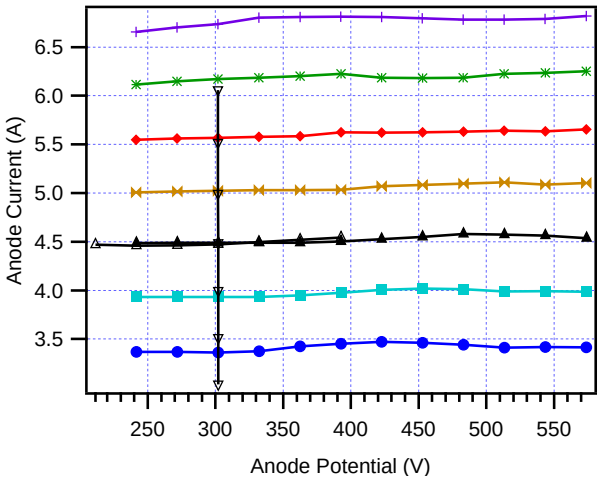

(b) Anode current vs. anode potential

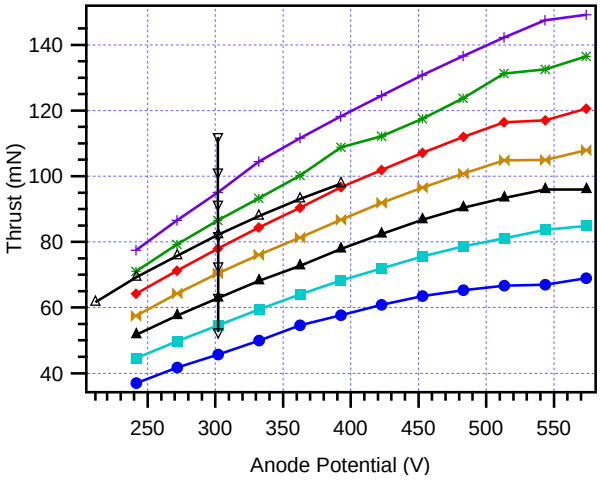

(c) Thrust vs. anode potential

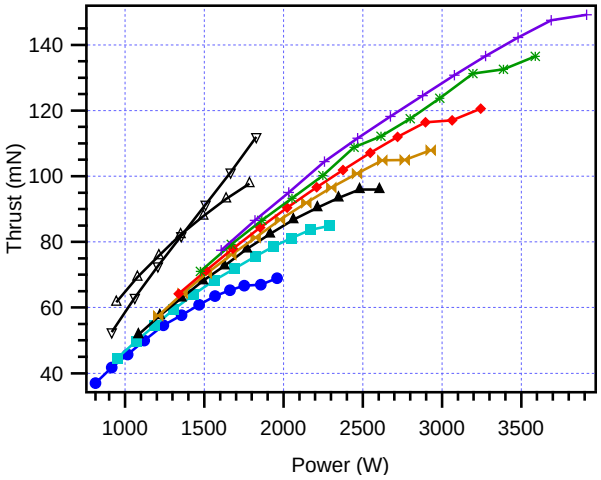

(d) Thrust vs. power

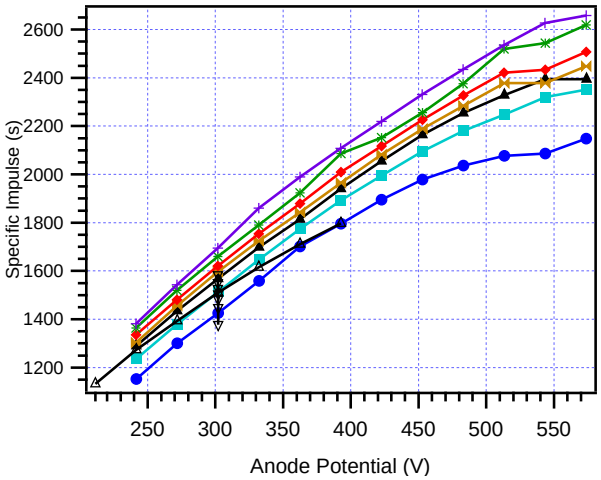

(e) Specific impulse vs. anode potential

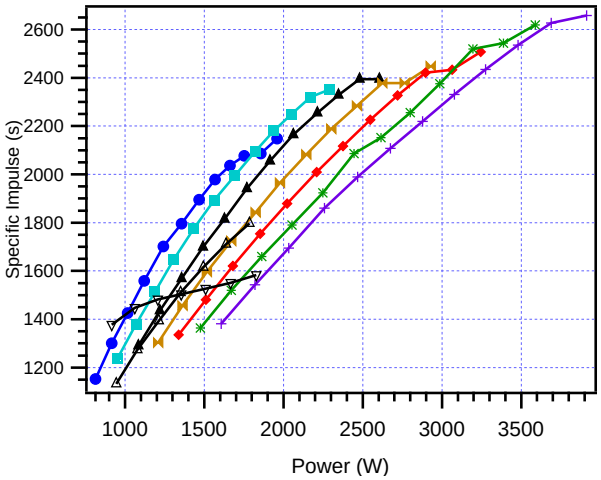

(f) Specific impulse vs. power

Figure 2. Thruster performance data from Ref. 1.

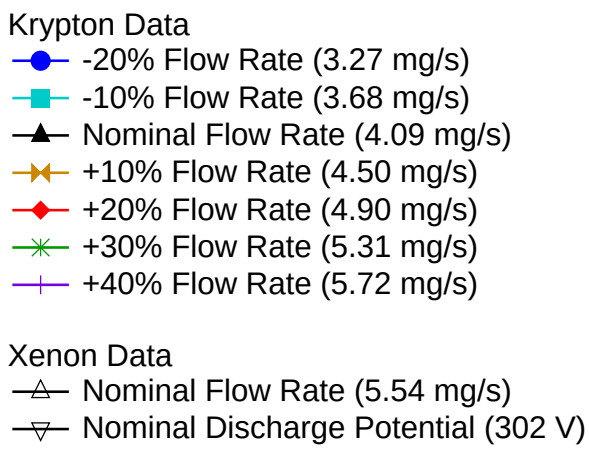

(a) Legend for performance plots.

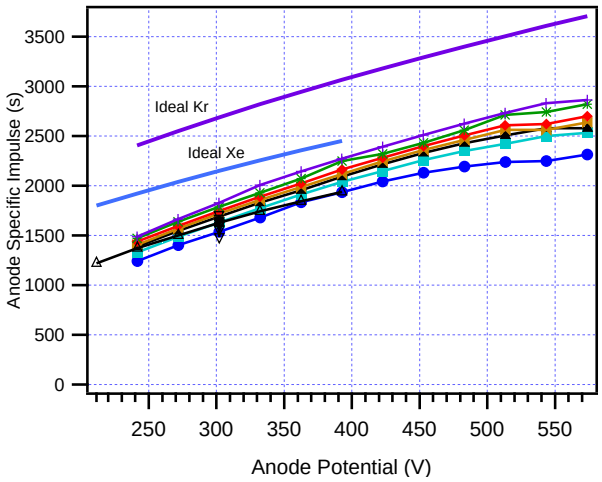

(b) Anode specific impulse vs. anode potential. Ideal values are shown for reference. (Note: Anode specific impulse calculation does not include cathode flow.)

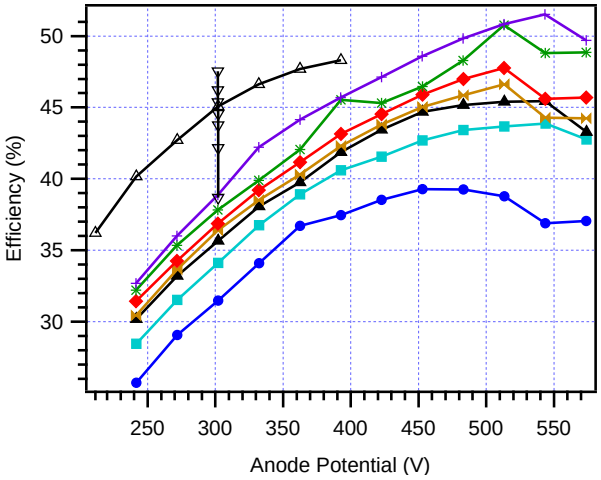

(c) Thrust efficiency vs. anode potential

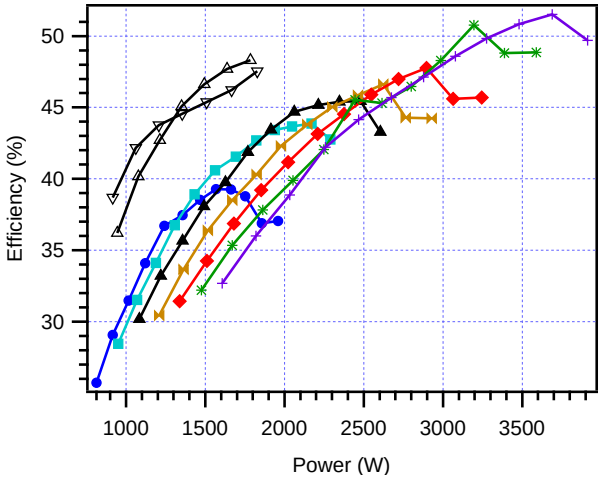

(d) Thrust efficiency vs. power

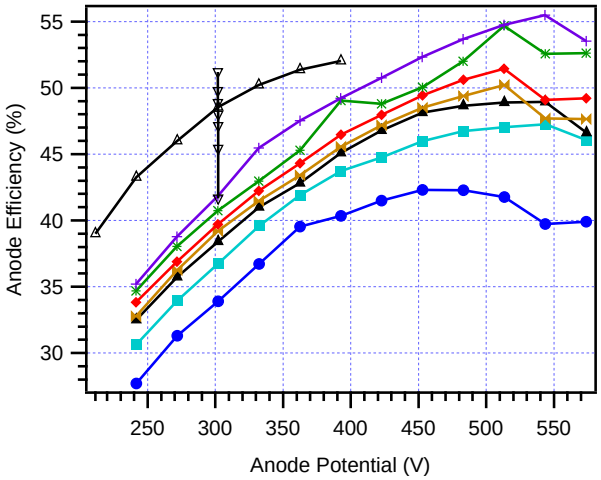

(e) Anode efficiency vs. anode potential (Note: Anode specific impulse calculation does not include cathode flow.)

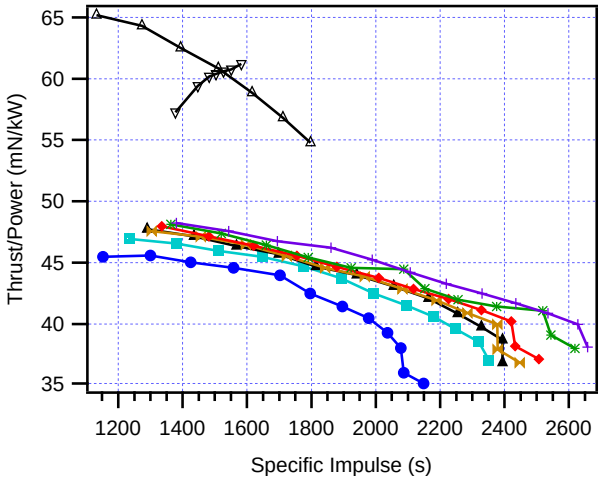

(f) Thrust to power ratio vs. specific impulse

Figure 3. Thruster performance data from Ref. 1 continued.

The 33rd International Electric Propulsion Conference, Washington D.C., United States, October 6-10, 2013
Distribution A: Approved for public release; distribution unlimited.

Parameter	Performance Testing	Life Testing
$\dot{m}_a$	4.17 mg/s	4.17 mg/s
$\dot{m}_c$	0.32 mg/s	0.32 mg/s
V_d	393 V	393 V
I_d	5.03 A	5.14 A
P	1977 W	2022 W
T	86.7 mN	-
I_{sp}	1966 s	-
η_t	0.423	-

Table 1. Thruster operating specifications.

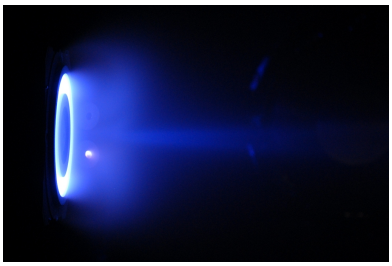

Figure 4. The SPT-100 firing at the beginning of the krypton life test.

Faraday Probe

Ion charge flux was measured throughout the life test using a guarded Faraday probe pictured in Fig. 1(b). The probe was mounted to a motion control system that allowed movement in polar coordinates. For these measurements, the probe remained at a radius of 100 cm and was swept between $\theta = \pm 90°$. The Faraday probe system was programmed to make a measurement sweep every 30 minutes. However, some Faraday probe sweeps did not occur during the first 50 h of the test due to software problems. Faraday probe measurements were used to approximate the ion beam current as

$$I_b \approx \pi r^2 \int_{-\frac{\pi}{2}}^{\frac{\pi}{2}} j(\theta)\,|\sin\theta|\mathrm{d}\theta \tag{1}$$

The Faraday electrodes were constructed from molybdenum. Ion current was collected with a disk measuring 8.3 mm in diameter. A concentric guard piece, measuring 22.5 mm in outer diameter, was used to minimize the effects of the plasma sheath on the ion current collector's effective collecting area. A 0.56 mm wide gap existed between the outer wall of the collector and the inner wall of the guard ring. The effective current collector area of the probe was calculated by adding a portion of the gap surface area to the collector surface area. The amount of gap area considered to contribute to the effective current collector area was proportional to the ratio of lateral wall surface area of the collector to the total lateral wall surface area on both sides of the gap as suggested in Ref. 18. Ion charge flux was measured by dividing the current to the collector by its effective surface area. The disk and guard ring were biased to -30 V with respect to chamber ground during the measurements so that ion saturation was achieved. The effects of secondary electron emission were assumed to be less than a few percent[19] and were neglected in the analysis of the measurements.

Optical Profilometer

A Microphotonics Nanovea optical profilometer (Fig. 5(a)) was used to measure erosion of the boron nitride insulators during the life test. The optical profilometry system combines a STIL CHR 150 confocal chromatic optical sensor, which measures the distance to a surface from an optical pen, a stepper motor driven sample positioning system, and a computer for setting up surface scans and recording the data. The non-contact

measurement technique of optical profilometers is commonly used for material science applications such as measuring microtopology and surface roughness. A previous study at AFRL used this profilometry system to measure the erosion of a divergent cusp-field thruster.[20]

The confocal chromatic optical sensor works by sending white light from a halogen bulb through an optical fiber to an optical pen (chromatic objective). As the light exits the pen it travels through a lens that creates a highly chromatically abberated beam where light focuses at different depths as a function of wavelength. When the beam hits the sample, light is reflected back through the optical pen and travels through the optical fiber. This backscattered light is diverted with a beam splitter to a pinhole that serves as a filter that allows focused light to pass through with high efficiency. The wavelength of the focused light is measured by a spectrometer. This wavelength corresponds to the distance between the chromatic objective and the surface.

The optical pen used for this study had 24 mm depth of field, a 3.0 μm depth accuracy, and a 50.0 μm lateral resolution. In a typical measurement configuration, the optical pen points normal to the sample surface and the plane of the motion control system. However, for the purpose of measuring the thruster channel geometry, the optical pen was mounted at an angle of 24.1° relative to vertical. As shown in Fig. 5(b), this mounting angle allowed optical access to the vertical walls of the insulators, but also necessitates the use of a coordinate transformation to interpret the data.

A polar coordinate motion control system consisting of a rotation stage and a linear stage was used for the surface scans of the SPT-100. Linear surface profile measurements spanning the diameter of the outer insulator were made in a spoke pattern around center of the thruster where the linear stage moved in increments of 0.10 mm. Profile measurements were made in angular increments of 2.5° from $\phi = 0$ to 357.5°. Figure 5(c) shows the orientation of the ϕ angular dimension within the thruster exit plane.

Each profilometry data set took 50 h to complete. Due to the tilt of the optical pen, only one interior side of the inner and outer channels were able to be scanned for a given direction of linear stage travel. To complete a linear profile for a given ϕ value, data from the scan 180° opposite in ϕ, where the linear stage traveled in the opposite direction relative to the thruster were added. Erroneous data points were filtered based on signal intensity and proximity to neighboring points to improve the quality of the measurements.

Testing History

The life test consisted of five separate firings of the thruster as listed in Table 2. Profilometry measurements were performed at the beginning of life (0 h), 100 h, and the end of the life test (205 h). During the life test, the chamber was only opened once to atmosphere (after 100 h of firing) so that the mid test profilometry measurement could be performed. However, between some firings the vacuum pumps were turned off and the chamber was at rough vacuum.

Dates (2012)	Duration (h)	Cumulative Time (h)
Sept. 7-10	74.35	74.35
Sept. 11-12	25.66	100.01
Sept. 18-19	31.37	131.37
Oct. 5-6	54.31	185.69
Oct. 8-9	19.33	205.01

Table 2. Five separate firings of the SPT-100 were performed to achieve a cumulative firing time of 205 h.

Results and Discussion

Anode Current and Faraday Probe Data

Throughout the life test, anode current data were collected at 0.5 Hz by the data acquisition system and Faraday probe sweeps were made every 30 minutes (excluding some time periods in the first firing). Figure 6 shows the anode current throughout the life test. Overall, the anode current remained steady at 5.1 A over the course of the life test with the constant propellant flow rate supplied by the digital mass flow controllers. A small increase in anode current was observed at the beginning of the firings, but would decay within a few

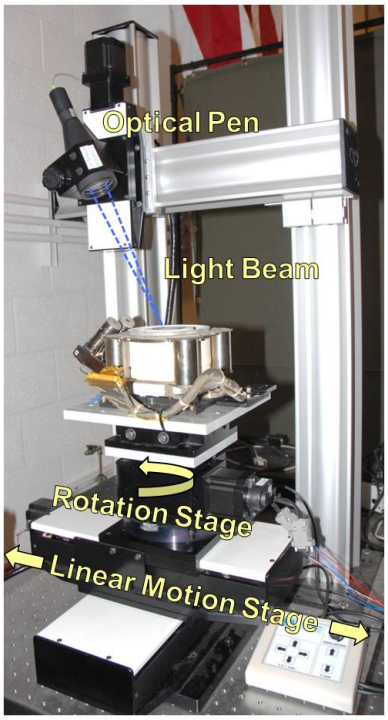

(a) Photograph of optical pen and motion control stages.

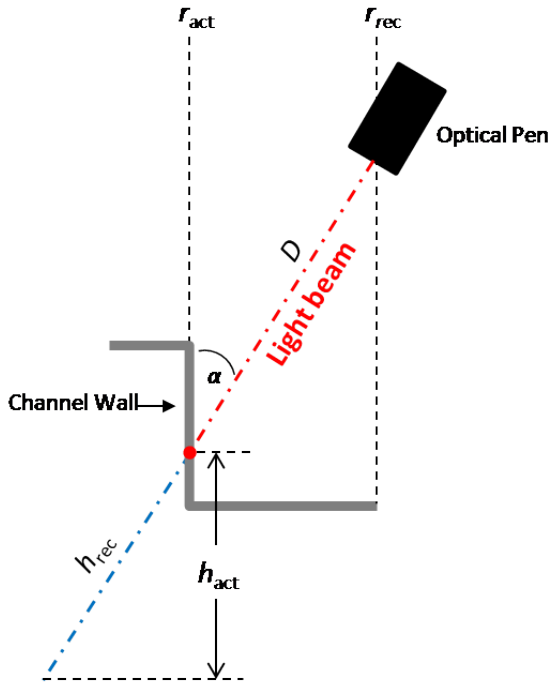

(b) Schematic of the tilted optical pen measurement geometry.

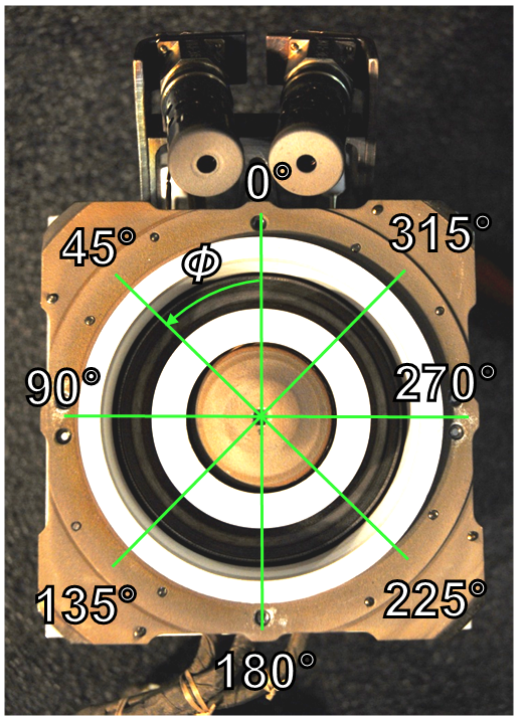

(c) Illustration of the locations of surface profile measurements. Measurements were taken in 2.5° increments of ϕ.

Figure 5. The implementation of the optical profilometer system for insulator erosion measurements.

hours. After 12 h of firing, momentary spikes in anode current began to occur. These spikes corresponded to hot, visibly glowing particles that were being expelled from the acceleration channel. These particles were thought to be graphite from the chamber walls redeposited on the interior of the thruster from ion beam sputtering. Figure 7 shows an oscilloscope trace of an individual current spike. The magnitude of the anode current spikes increased over time for the first 100 h of firing. When the chamber was open after 100 h, a thick film of graphite was observed on the center pole and a thin film was seen in the channel interior (Fig. 9(e)). However, for the second half of the life test, the current spikes became less frequent and much of the deposited graphite film on the center pole was missing when the chamber was opened at the end of the test (Fig. 9(f)).

Faraday probe data are also plotted in Fig. 6. Ion beam current was integrated from the Faraday probe sweeps and was observed to correspond to the small trends in the anode current. Its average value was 4.93 A over the course of the life test. Ion charge flux at $\theta = 0$, 15, and 30° were also plotted with time to show any changes in the shape of the beam. Figure 8 shows charge flux data from the Faraday probe at various times throughout the life test. These plots show that the beam remained nearly constant in angular distribution over the course of the test.

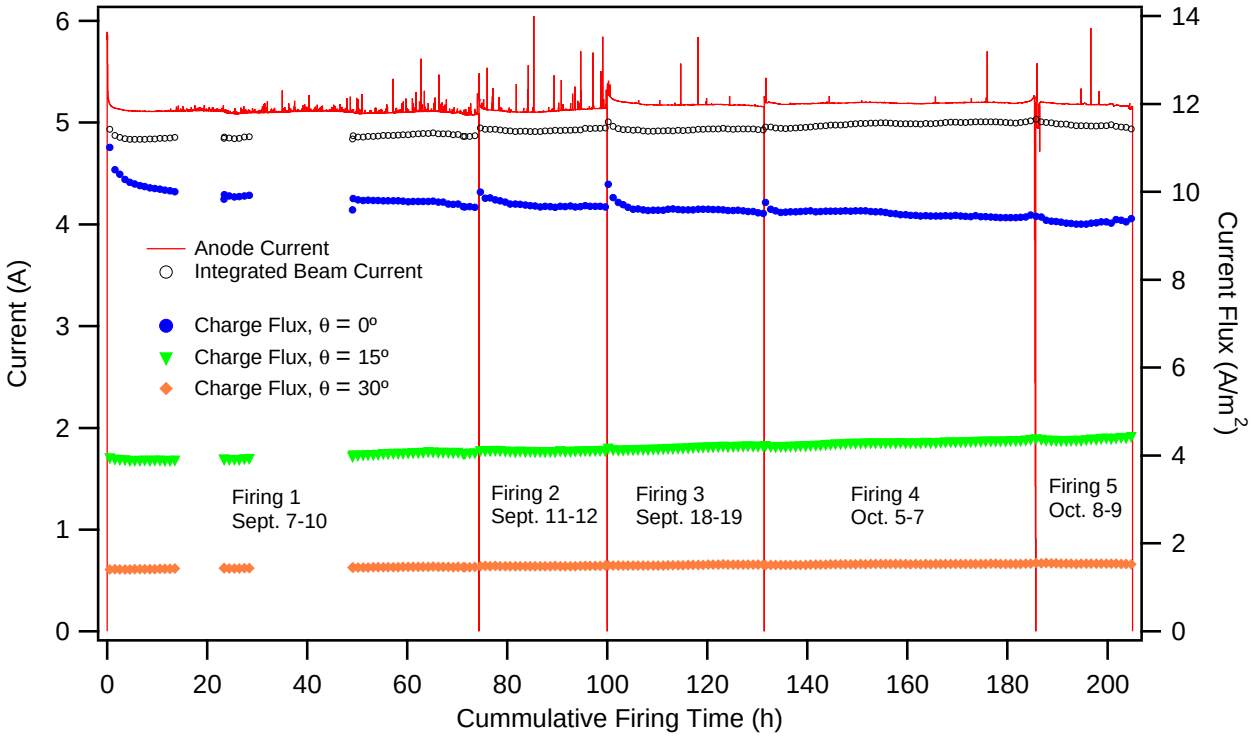

Figure 6. Anode current, integrated beam current, and ion charge flux throughout the life test.

Erosion Data

Optical profile measurements were taken after 0, 100, and 205 h of thruster firing. An alignment bracket for the thruster mount was created on the profilometer motion system to ensure a repeatable remounting position of the thruster between firings. Also, care was taken to avoid moving any parts of the system or resetting the motion control coordinates between measurements. Figure 9 shows the thruster's appearance at each of these measurement times. As seen in Figs. 9(e) and 9(f), significant graphite deposition occurred in the channel and on the center magnetic pole covering. In the acceleration channel, a distinct boundary formed between the regions of graphite accumulation and insulator erosion where the boron nitride remained clean. The optical sensor of the profilometer was configured with a measurement frequency to obtain an optimized signal on clean, white boron nitride surfaces and sufficient signal was obtained for all three data sets for these surfaces. However, the optical sensor received a weak signal while the beam was located on the graphite coated surfaces and often failed to record a measurement. This minor issue made resolving

The 33rd International Electric Propulsion Conference, Washington D.C., United States, October 6-10, 2013

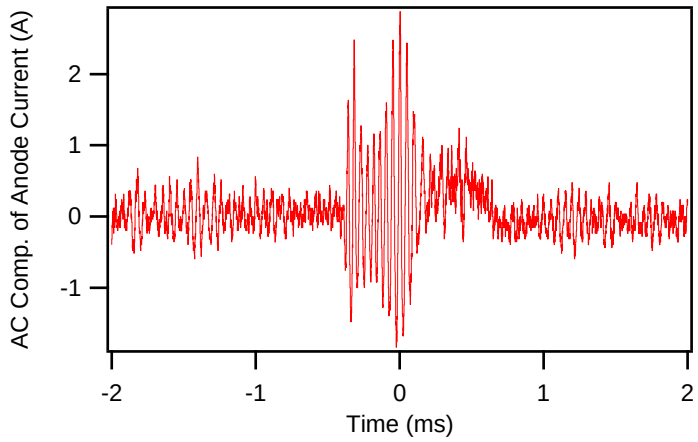

Figure 7. An anode current spike due to a graphite ember being expelled from the acceleration channel.

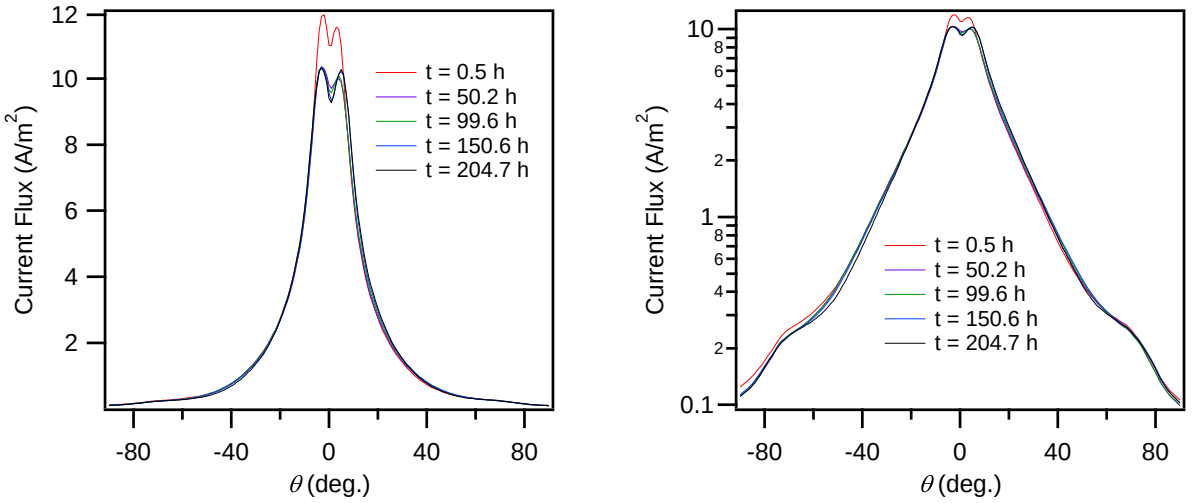

(a) Linear plot of Faraday probe data.

(b) Log scale plot of Faraday probe data.

Figure 8. Faraday probe sweeps were taken every half hour throughout the life test. The charge flux profile remained nearly constant over the full duration. Small temporary increases in charge flux were observed after thruster ignition.

the transition between erosion and deposition more difficult. Partially loose flakes of graphite also obscured some surface features at the transition.

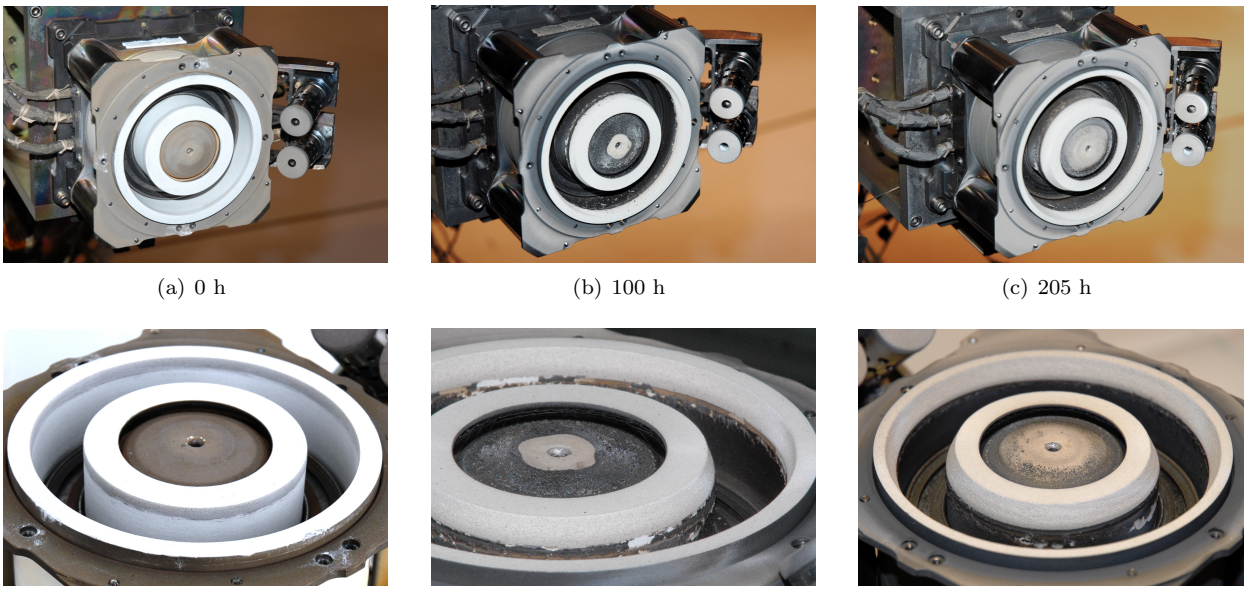

(a) 0 h (b) 100 h (c) 205 h

(d) 0 h (e) 100 h (f) 205 h

Figure 9. Photos of the SPT-100 at beginning of life and after 100 and 205 h of firing.

A comparison of the erosion profile measurements for each time at $\phi = 0°$ is shown in Fig. 10. To calculate changes in insulator radius, smoothing splines were fitted to the walls of the channels and subtracted from splines from earlier profile measurements as illustrated in Fig. 11. Insulator erosion is plotted as a function of channel depth relative to the exit plane in Fig. 12. Profiles for every ϕ position are plotted to show the spread of the results. Also shown is the mean erosion profile with error bars that display ± 1 standard deviation. The erosion for the inner and outer insulators was almost identical at both 100 and 205 h. Figure 13 shows that the mean inner and outer insulator erosion profiles varied less than 0.1 mm throughout the depth range.

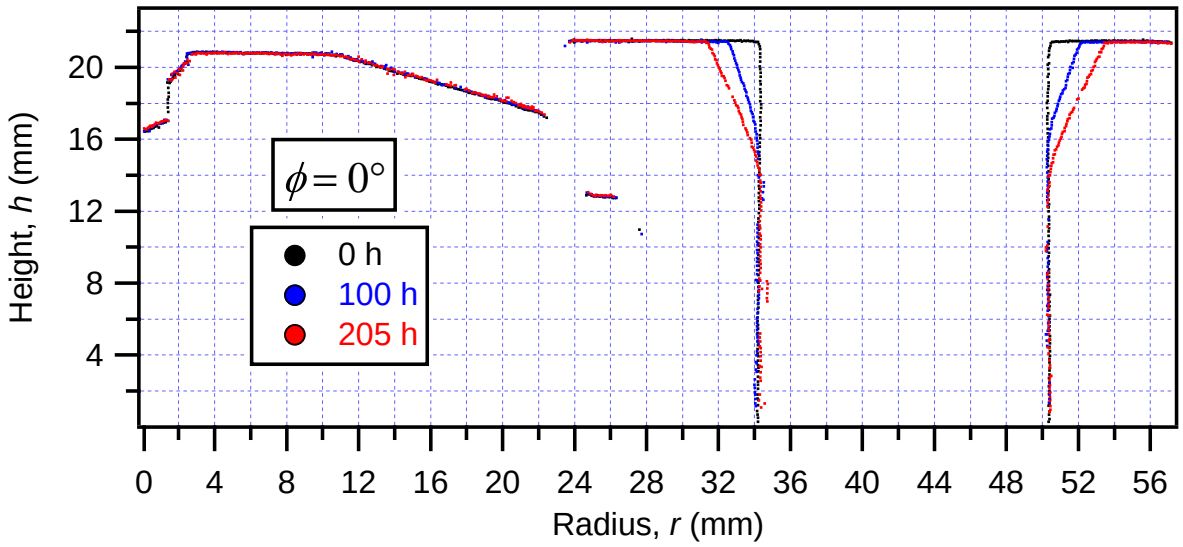

Figure 10. A comparison of erosion profiles for $\phi = 0°$

If the erosion of the insulators had any trends as a function of azimuth angle, they were smaller than what could be detected with the uncertainty of this experiment. Figure 14 shows the azimuthal variation in

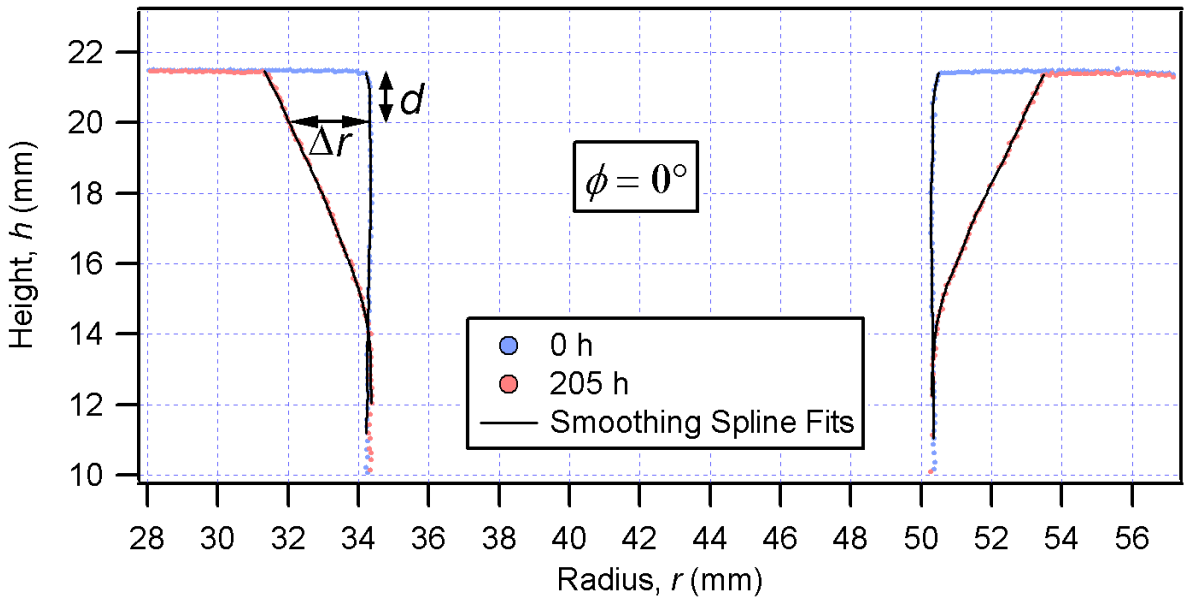

Figure 11. Smoothing splines were fit to the channel walls as a step in the calculation erosion. Erosion was measured in the radial direction as Δr and was recorded as a function of depth relative to the exit plane, d.

erosion at different channel depths. The result show an out-of-phase sinusoidal pattern between the inner and outer insulator erosion where the phase constant changes for the two measurement times. This result is believed to be non-physical and caused by small errors among the radial coordinates in the data sets. This plot points out the limitations of the measurement technique used in this study. Although the optical detector of the spectrometer has a depth accuracy of 3.0 μm, the main source of experimental error lies with the consistency of the coordinates of the data among the different sets and within the same set. Remounting of the thruster, hysteresis in stepper motor position, the larger than ideal linear step resolution (0.1 mm in these tests), and small drifts in the relative depth coordinate of the optical pen during the weeks between data sets all add uncertainty in position. The fact that the erosion profiles for the various angles all have the same shape but are slightly offset from each other is consistent with the idea that there were some offsets in the radial coordinates between data sets. Given the spread in the similarly shaped erosion profiles, the standard deviation of the distribution was used to estimate the uncertainty of the mean profile, which was considered to be a good representation of the bulk data set.

The erosion profiles were used to calculate the average erosion rates for the firing time increments as shown in Fig. 15. The erosion rate as a function of channel depth is constantly changing as the erosion progresses. The erosion rate was always greatest at the exit plane for both time periods, but for the later firing, erosion rate increased for points greater than 2 mm deep in the channel while decreasing for shallower depths.

A 7,000 hour life test of the SPT-100 operating at its nominal xenon condition is described in Ref. 21. This paper presents insulator erosion profiles of the SPT-100 at 7,000 h along with erosion profiles of the M100 thruster at different time intervals up to 4,100 h. The M100 and SPT-100 are analogous thrusters where the later has modifications to meet western flight standards. Erosion profiles of the M100 at 160 h, 310 h, and 600 h were used for comparison with the present data and are plotted in Fig. 17. The parameters of energy throughput and total impulse delivered were calculated for each erosion profile based on the average performance and thruster telemetry provided. These parameters are useful as a basis of comparison for these life tests performed at different power levels. The 160 h and 310 h xenon profiles coincidently have similar energy throughput values to the krypton profiles enabling a direct comparison for this parameter. The erosion profiles shapes are noticeably different between these tests. The krypton profiles exhibit a steeper erosion profile where a greater proportion of the erosion is concentrated at shallow depths compared to the xenon profiles. The 160 h xenon profile shows about the same amount of erosion at exit plane as the 100 h krypton profile, but more erosion at points deeper in the channel. The 205 h krypton profile shows a little

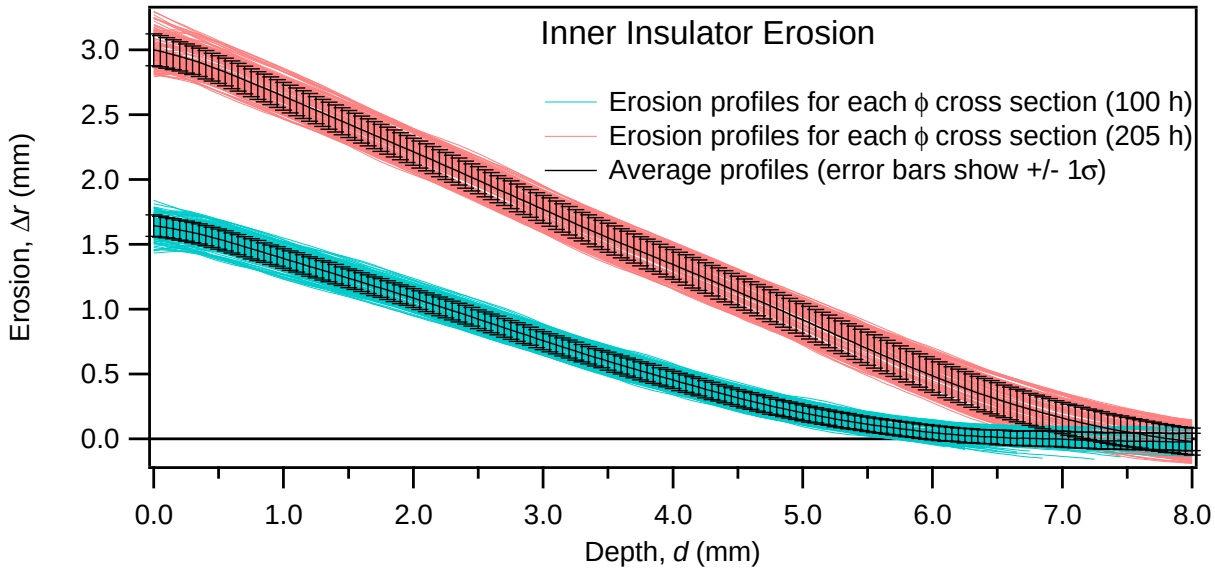

(a) Inner insulator erosion profile.

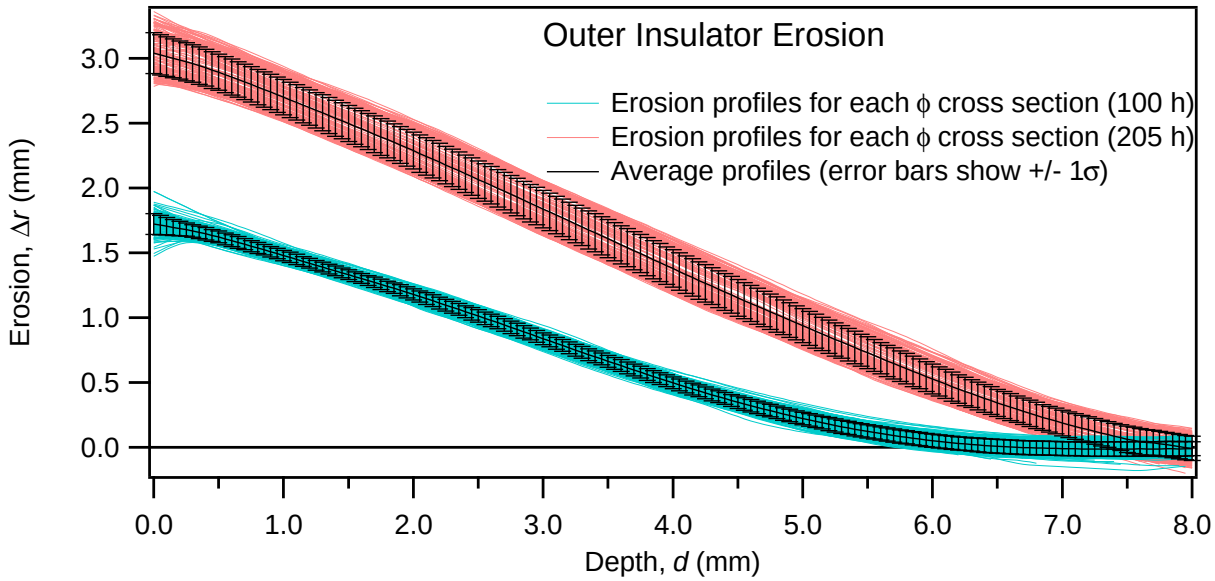

(b) Outer insulator erosion profile.

Figure 12. Insulator erosion profiles. Cross-section measurements were made every $\phi = 2.5°$. The set of measurements is plotted along with the average erosion profile. Error bars show ± 1 standard deviation.

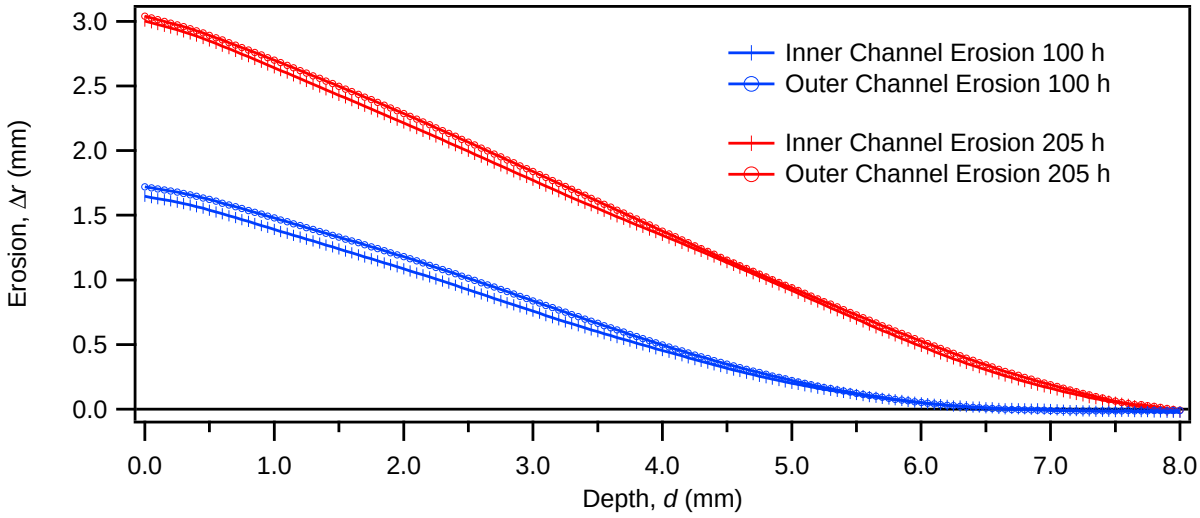

Figure 13. A comparison of the inner and outer erosion profiles shows they are nearly identical.

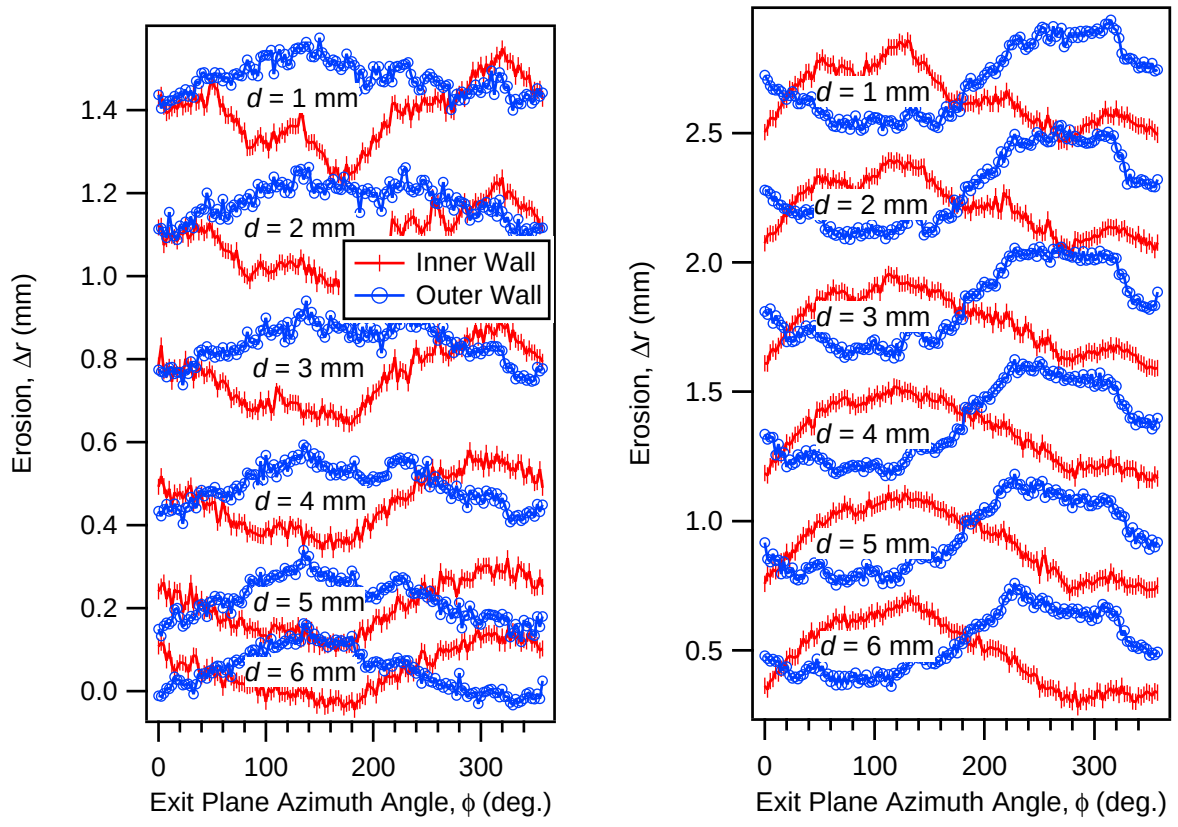

(a) 100 h

(b) 205 h

Figure 14. Azimuthal variation in measured erosion at various channel depths. The periodic, out-of-phase variation in erosion between the inner and outer insulators suggests that this effect could be the result of a small discrepancy in the radial coordinate between each data set. The variations in the data were no larger than the experimental uncertainty.

The 33rd International Electric Propulsion Conference, Washington D.C., United States, October 6-10, 2013

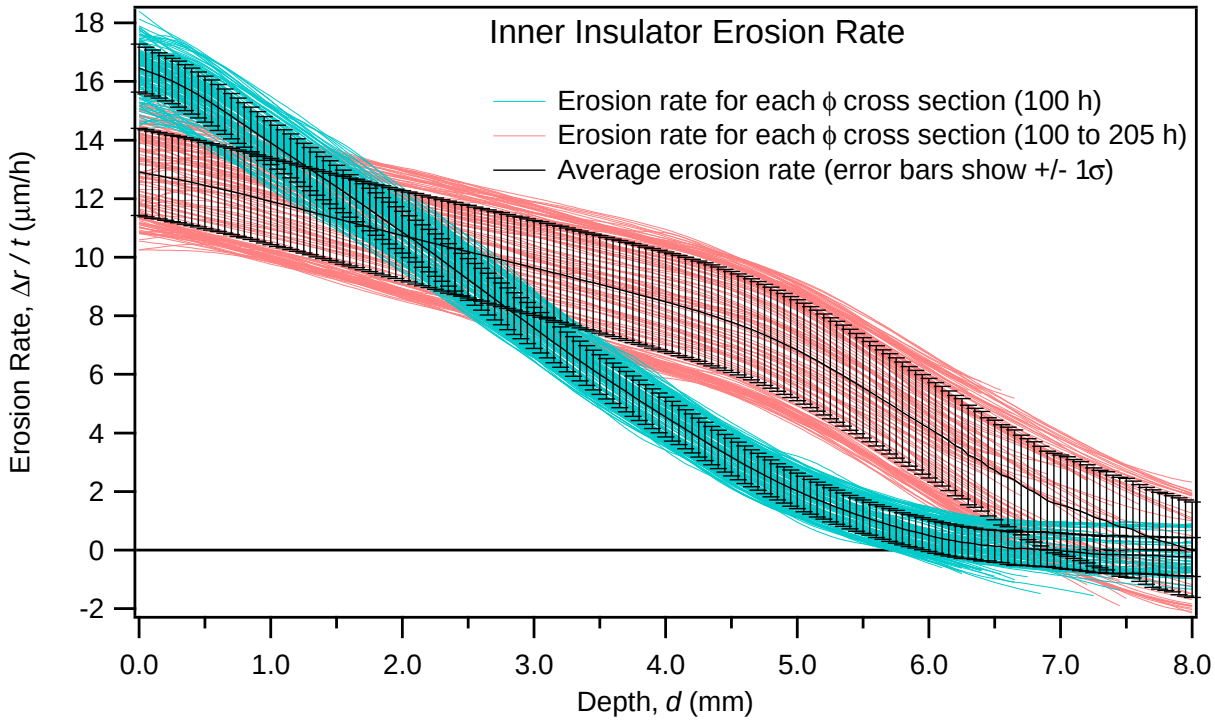

(a) Inner insulator erosion rate.

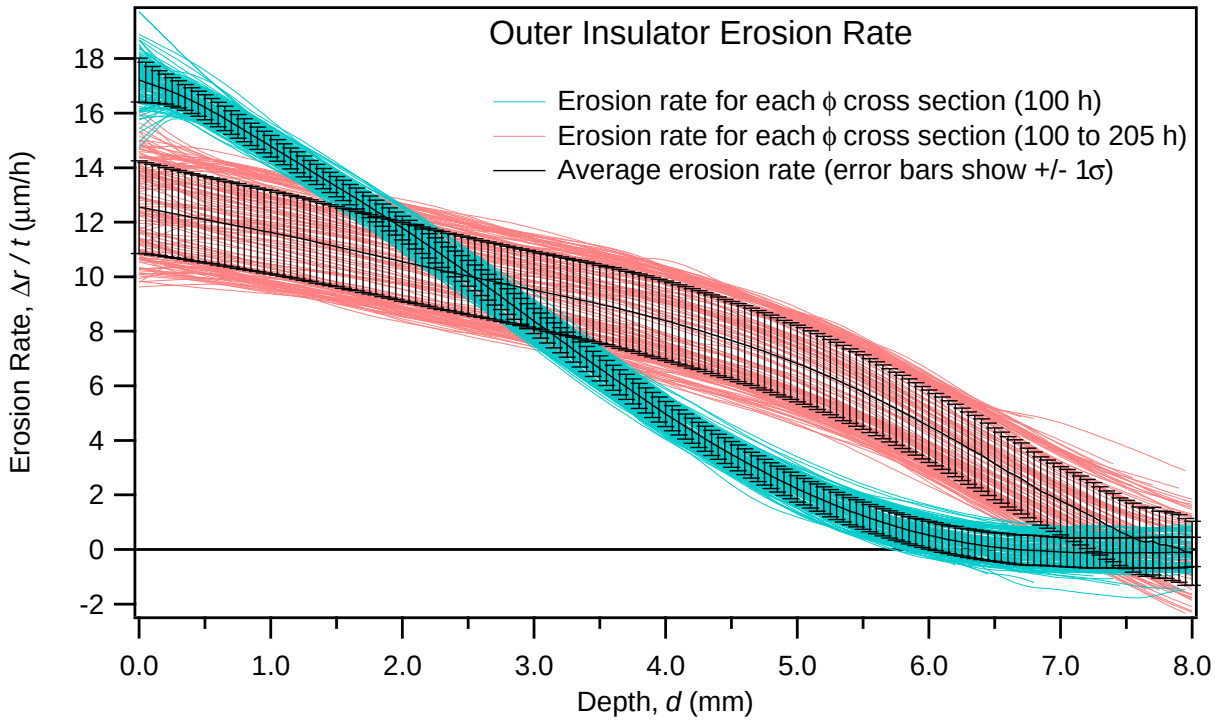

(b) Outer insulator erosion rate.

Figure 15. Insulator erosion rate profiles. Cross-section measurements were made every $\phi = 2.5°$. The set of measurements is plotted along with the average erosion rate profile. Error bars show ± 1 standard deviation.

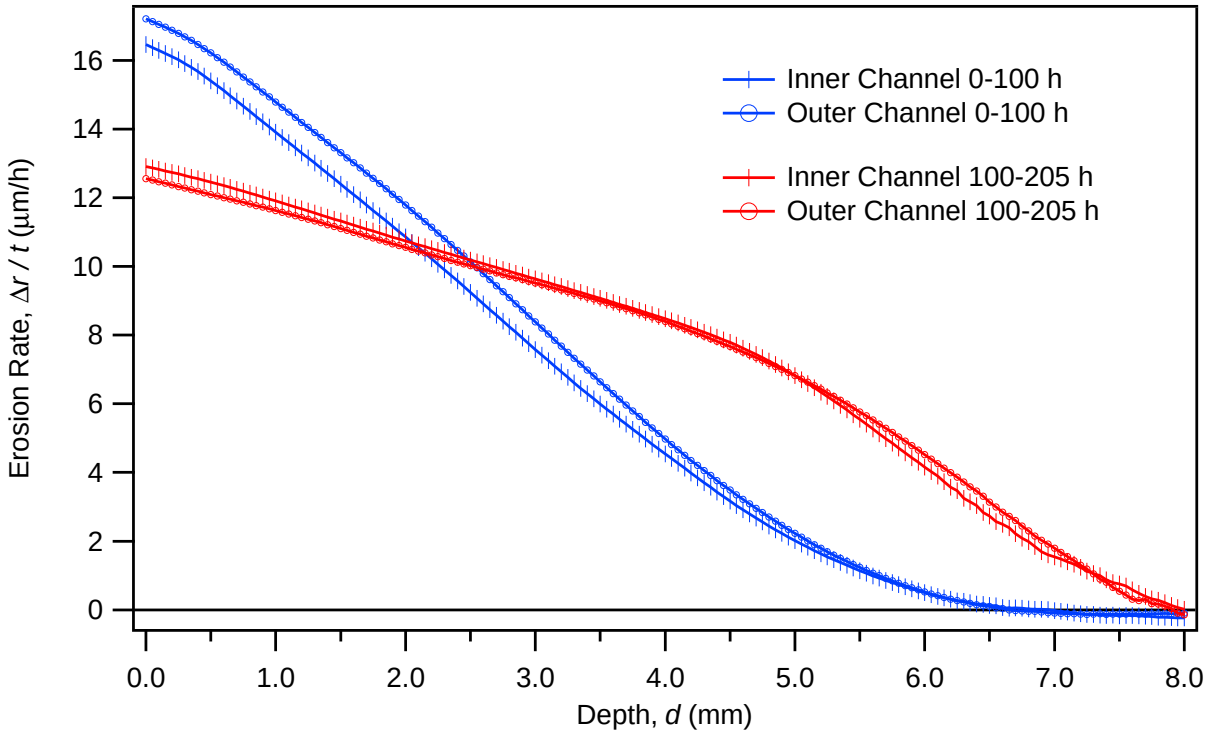

Figure 16. A comparison of the inner and outer erosion rate profiles shows they are nearly identical.

less erosion overall than the 310 h xenon profile, but more erosion at the exit plane.

Conclusions

The 205 h krypton life test of the SPT-100 demonstrated the capability of the thruster to operate at a 50% higher than nominal power for an extended duration while maintaining a steady discharge current and ion beam charge flux profile. The erosion profiles measured in this study have shown that optical profilometry is a useful experimental technique for measuring boron nitride insulators in Hall thruster life testing.

From the data gathered in this short life test, it was unclear if the thruster life time at this operating condition would be meet the 5,860 hour mark required for NSSK in the example geosynchronous communications satellite mission. The amount of energy throughput for 5,860 hours of firing time with this krypton condition is the same amount as 8,800 hours of nominal xenon operation. The SPT-100 is considered capable of firing for 9,000 h at nominal conditions.[17,14] If insulator erosion roughly scales with energy throughput as the erosion profile comparison suggests, then it might be possible for the thruster to endure the mission at the krypton operating condition. However, for any serious attempts to use a krypton as a propellant, long duration life tests would be required to prove the thruster's endurance.

Published Hall thruster erosion data is in limited supply and erosion data with alternative propellants is extremely rare. These measurements provided some basic data to characterize the initial phases of boron nitride insulator erosion from krypton propellant.

Acknowledgments

The authors would like to thank D. Luke O'Malley, Landon Tango, and Joseph Blakely for their assistance in exploring and implementing various experimental techniques using the optical profilometer. Technical advice from Stephen Gildea on evaluating profilometer data was appreciated. Thanks also go to Ken Unfried from Linde Specialty Gases for providing references and information about the rare gas market.

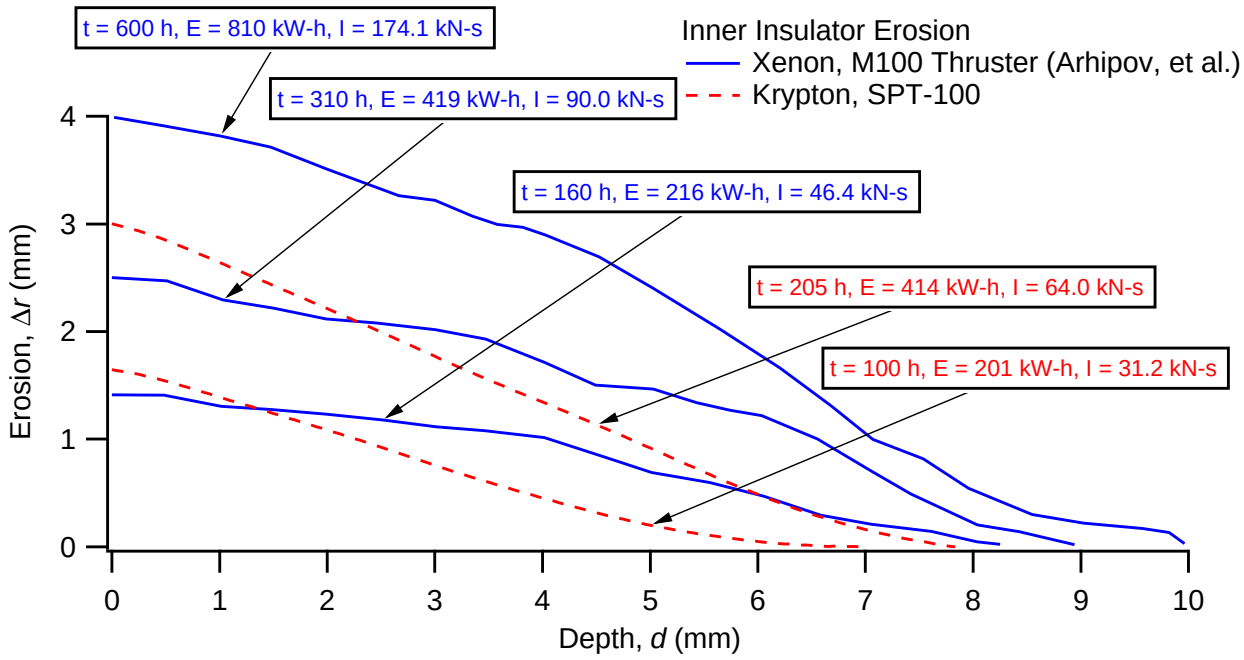

(a) Inner insulator: Comparison of xenon and krypton erosion data.

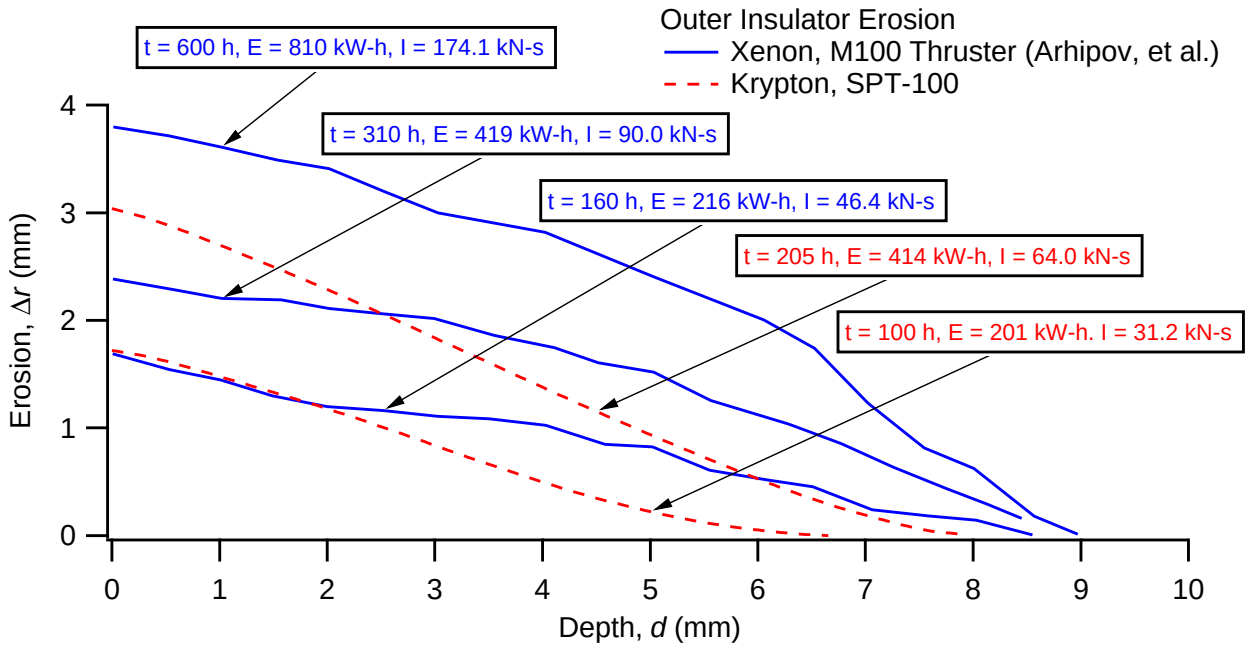

(b) Outer insulator: Comparison of xenon and krypton erosion data.

Figure 17. Comparison of insulator erosion from xenon and krypton propellant. The xenon erosion data is from a 4,100 h life test at nominal conditions in Ref. 21. Each trace is labeled by burn time, energy throughput, and impulse delivered.

Appendix: Krypton Mission Example

A simplified example mission was studied to evaluate the possibility of using krypton propellant for the flight model SPT-100 on a spacecraft based on the performance measurements in this study. This example mission was intended to replicate the general requirements of a propulsion system for north-south station keeping on a communications satellite in geosynchronous orbit. In this example, the spacecraft would have the following characteristics and requirements:

- Initial spacecraft mass: 3760 kg
- Mission lifetime: 15 years
- Thruster cant angle: 40 ° (directional cosine loss)
- Quantity of SPT-100 thrusters: 2
- Delta-V required: (51 m/s/year)×15 years = 765 m/s

The propellant mass required for this mission can be calculated from the basic rocket equation as:

$$M_p = M_0 - M_0 \exp\left(\frac{-\Delta V}{g_e I_{\mathrm{sp}} \cos\theta}\right) \tag{2}$$

The resulting propellant mass for the mission is divided between the two thrusters. The number of required operational hours for each thruster is determined by dividing the propellant mass for each thruster by the propellant flow rate for its operating condition. The results of this analysis are plotted in Fig. 18.

In Fig. 18. propellant mass per thruster is plotted versus the required operational time per thruster for the matrix of krypton operating conditions tested. Operating condition data points fall along lines of propellant flow rate. Linear interpolation was used to create contours for the operational power required per thruster for krypton propellant. As propellant mass and operational time requirements decrease, the power requirement increases. The tested xenon operating conditions are also displayed for reference.

A mission using xenon at the nominal operating condition (1356 W) would require 6,160 h of operational time per thruster and 120 kg of propellant per thruster. This condition is marked for reference on the plot. The data for xenon operating with the nominal discharge potential as propellant flow rate varies is marked with a red line. This forms a boundary for operating conditions that would have a propellant mass savings relative to xenon operating at its nominal discharge voltage. Tests have validated the SPT-100 life time as exceeding 2.71 million N-s (equivalent to approximately 9,000 hours of operational time) for xenon at the nominal condition.[17,14] This boundary is also marked in red for reference. Some krypton operating conditions within these boundaries may be feasible for completing this mission. Although it should be noted that most of these krypton cases require a significantly higher power throughput than the life tested nominal xenon condition and thus may limit the lifetime of the thruster to values lower than the validated xenon figure. Thruster erosion rates with krypton are unknown so life testing would be required to determine reasonable operational times.

One krypton operating condition that may be appropriate is the 390 V, nominal flow rate setting. Using this setting, 54 kg of total propellant mass could be saved relative to the nominal xenon operating condition. However, 400 W of extra power per thruster and an extra 400 hours of firing time for each thruster would be required. It should be noted that off-nominal condition xenon cases could be chosen for fuel savings and they would offer better overall performance than the krypton operating conditions studied. As seen in the performance data, the krypton operating conditions did not offer significantly better specific impulse than xenon so choosing krypton propellant for potential mass savings may not be a good idea. Also, krypton propellant has a higher tankage fraction and may require larger or more massive tanks for storage. The potential benefit krypton propellant could offer would be its cheaper price.

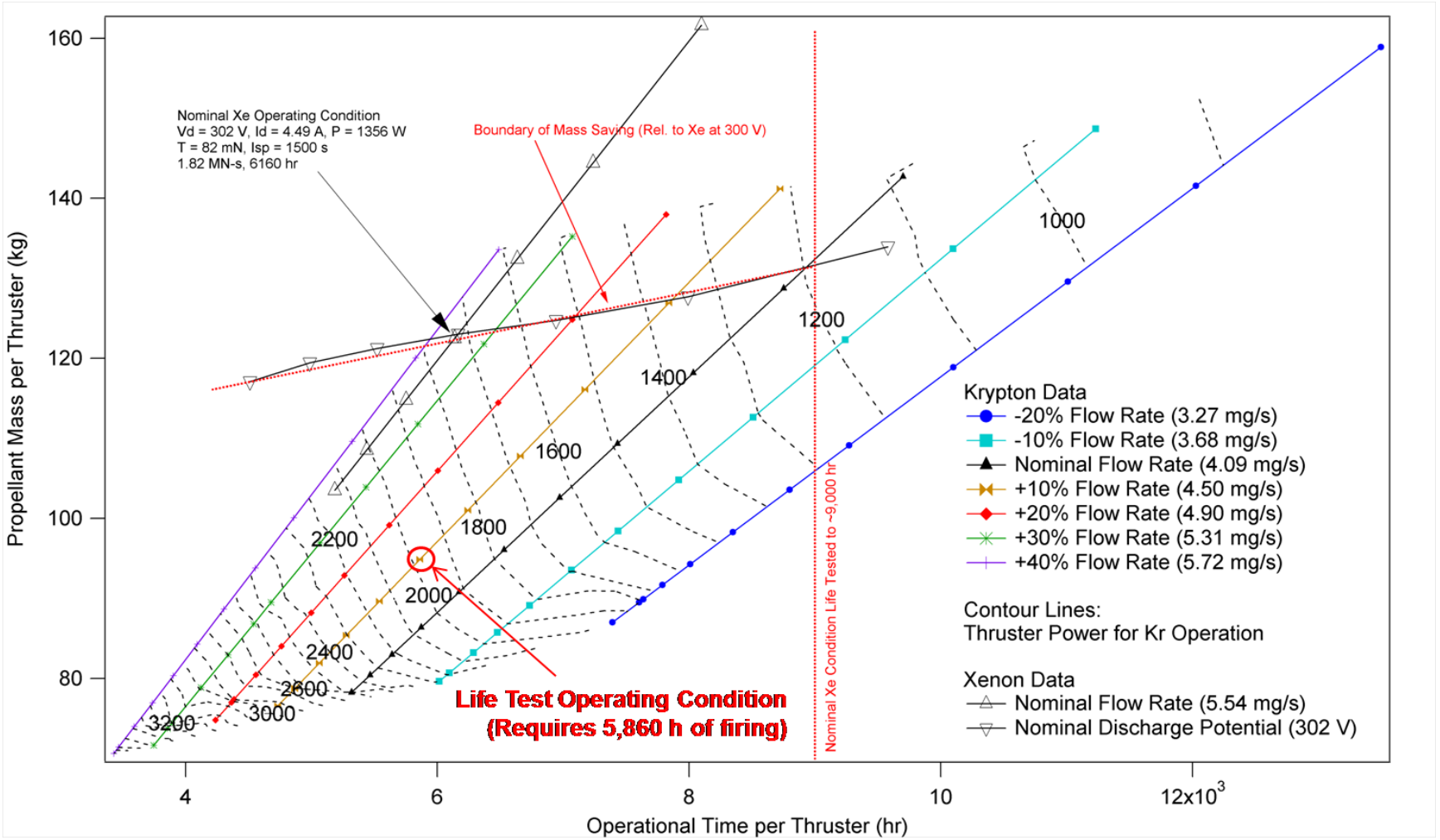

Figure 18. Simplified mission analysis for an SPT-100 propulsion subsystem with two thrusters operating on krypton propellant for north-south station keeping. In this example, the spacecraft has an initial mass of 3760 kg and a lifetime delta-V requirement of 765 m/s.

References

[1]Nakles, M. R., Hargus Jr., W. A., Delgado, J. J., and Corey, R. L., "A Performance Comparison of Xenon and Krypton Propellant on an SPT-100 Hall Thruster," *Proceedings of the 32nd International Electric Propulsion Conference*, Weisbaden, Germany, September 2011, IEPC-2011-003.

[2]Duchemin, O., Valentian, D., and Cornu, N., "Cryostorage of Propellants for Electric Propulsion," *45th AIAA/ASME/SAE/ASEE Joint Propulsion Conference, No. AIAA-2009-4912*, Denver, CO, 2009.

[3]Betzendahl, R., "Ever Changing Rare Gas Market," *CryoGas International*, Februrary 2013.

[4]Linnell, J. A. and Gallimore, A. D., "Efficiency Analysis of a Hall Thruster Operating with Krypton and Xenon," *Journal of Propulsion and Power*, Vol. 22, No. 6, November-December 2006, pp. 1402–1412.

[5]Kim, V., Popov, G., Kozlov, V., Skrylnikov, A., and Grdlichko, D., "Investigation of SPT Performance and Particularities of its Operation with Kr and Kr/Xe Mixtures," *In the Proceedings of the 27th Electric Propulsion Conference*, No. IEPC-01-065, 2001.

[6]Marrese, C., Haas, J. M., Domonkos, M. T., Gallimore, A. D., Tverdokhlebov, S., and Garner, C. E., "The D-100 performance and plume characterization on krypton," *Proceedings of the 32nd AIAA/ASME/SAE/ASEE Joint Propulsion Conference and Exhibit*, No. AIAA 96-2969, 1996.

[7]Jacobson, D. T. and Manzella, D. H., "50 kW Class Krypton Hall Thruster Performance," *In the Proceedings of the 39th AIAA/ASME/SAE/ASEE Joint Propulsion Conference*, No. AIAA 2003-4550, 2003.

[8]Arkhipov, B., Koryakin, A., Murashko, V., Nesterenko, A., Khoromsky, I., Kim, V., Kozlov, V., Popov, G., and Skrylnikov, A., "The Results of Testing and Effectiveness of Kr-Xe Mixture Application in SPT," *In the Proceedings of the 27th International Electric Propulsion Conference*, No. IEPC-01-064, 2001.

[9]Arkhipov, B., Khoromsky, I., and Murashko, V., "Problems of designing EPSs with SPTs Working on Krypton-Xenon Mixture," *Proceedings of the 38th AIAA/ASME/SAE/ASEE Joint Propulsion Conference and Exhibit*, No. AIAA-2002-3682, 2002.

[10]Welle, R., "Xenon and Krypton Availability for Electric Propulsion: An Updated Assessment," *Proceedings of the AIAA/SAE/ASME/ASEE 29th Joint Propulsion Conference and Exhibit*, July 1993, AIAA 1993-2401.

[11]Nakles, M. R., Hargus Jr., W. A., Delgado, J. J., and Corey, R. L., "A Performance and Plume Comparison of Xenon and Krypton Propellant on an SPT-100 Hall Thruster," *Proceedings of the AIAA/ASME/SAE/ASE 48th Joint Propulsion Conference and Exhibit*, July 2012, AIAA-2012-4116.

[12]Garner, C. E., Brophy, J. R., Polk, J. E., and Pless, L. C., "Cyclic Endurance Test of a SPT-100 Stationary Plasma Thruster," *In the Proceeding of the 30th AIAA/SAE/ASME/ASEE Joint Propulsion Conference and Exhibit*, 1994, AIAA-94-2856.

[13]Sankovic, J. M., Hamley, J. A., and Haag, T. W., "Performance evaluation of the Russian SPT-100 thruster at NASA LeRC," *Proceedings of the 23rd International Electric Propulsion Conference*, 1993, IEPC-93-094.

[14]Corey, R. L., Gascon, N., Delgado, J. J., Gaeta, G., Munir, S., and Lin, J., "Performance and Evolution of Stationary Plasma Thruster Electric Propulsion for Large Communications Satellites," *Proceedings of the 28th AIAA International Communications Satellite Systems Conference*, No. AIAA 2010-8688, 2010.

[15]Summers, R., "Empirical Observations on the Sensitivity of Hot Cathode Ionization Type Vacuum Gages," Tech. rep., NASA, 1969, NASA-TN-D-5285.

[16]Kim, V., Kozlov, V., Semenov, A., and Shkarban, I., "Investigation of Boron Nitride Based Ceramics Sputtering Yield Under its Bombardment by Xe and Kr Ions," *Proceedings of the 27th International Electric Propulsion Conference*, Pasadena, CA, October 2001.

[17]Gnizdor, R., Kozubsky, K., Koryakin, A., Maslennikov, N., Pridannikov, S., and Day, M., "SPT100 Life Test with Single Cathode up to Total Impulse Two Million Nsec," *Proceedings of the 36th AIAA/ASME/SAE/ASEE Joint Propulsion Conference and Exhibit*, No. AIAA-98-3790, 1998.

[18]Brown, D. L., *Investigation of Low Discharge Voltage Hall Thruster Characteristics and Evaluation of Loss Mechanisms*, Ph.D. thesis, University of Michigan, 2009.

[19]Brown, S. C., *Basic Data of Plasma Physics*, American Institute of Physics Press, New York, 1994.

[20]Gildea, S. R., Matlock, T. S., Martinez-Sanchez, M., and Hargus, Jr., W. A., "Erosion Measurements in a Low-Power Cusped-Field Plasma Thruster," *Journal of Propulsion and Power*, Vol. 29, No. 4, July-August 2013, pp. 906–918.

[21]Arhipov, B. et al., "The Results of 7000-Hour SPT-100 Life Testing," *Proceedings of the 24th International Electric Propulsion Conference*, Moscow, Russia, September 1995, IEPC-95-39.

A 205 Hour Krypton Propellant Life Test of the SPT-100 Operating at 2 kW

M.R. Nakles
ERC, Inc.
Spacecraft Propulsion Branch
Edwards Air Force Base, CA

W.A. Hargus, Jr.
Air Force Research Laboratory
Spacecraft Propulsion Branch
Edwards Air Force Base, CA

Jorge J. Delgado and Ronald L. Corey
Space Systems/Loral
Palo Alto, CA

Introduction

- **Kr is a less costly propellant alternative to Xe**
  - 10x cheaper by vol., 6x cheaper by mass
  - Lower thruster efficiency due to lower propellant utilization fraction
- **Kr performance measurements performed at AFRL**
  - Conditions ranging from 800 W to 3.9 kW tested
  - Kr performs better for higher discharge powers than at nominal power (1350 W)
- **Hall thruster erosion data with krypton propellant is rare**
  - Use of Kr on mission would necessitate longer firing times and/or higher power operating conditions
  - With more energy throughput, boron nitride insulators may not endure the mission duration
  - One study* reports a 30-50% smaller sputtering yield for boron nitride bombarded by Kr compared to Xe at a given energy

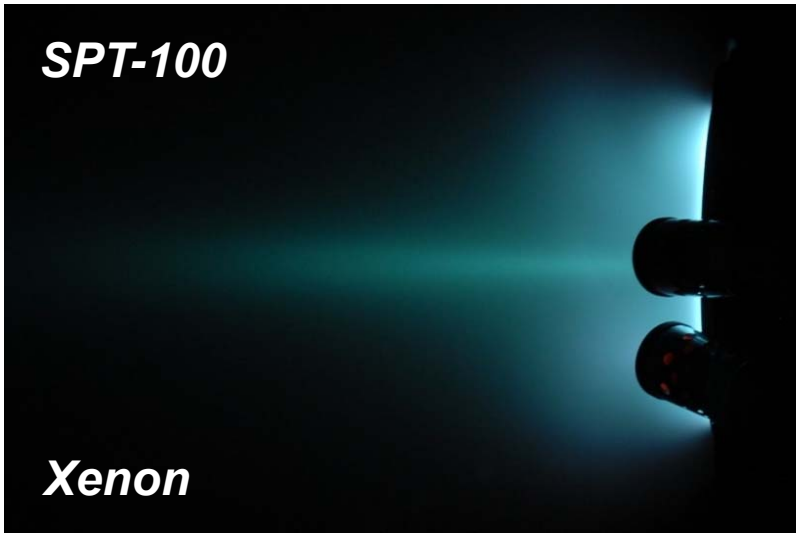

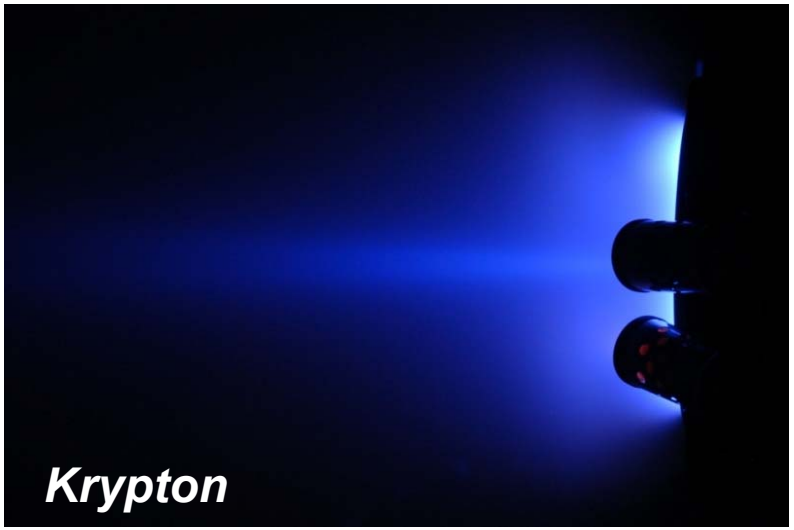

*Kim, V., et. al. "Investigation of Boron Nitride Based Ceramics Sputtering Yield Under its Bombardment by Xe and Kr Ions," Proceedings of the 27th International Electric Propulsion Conference, Pasadena, CA, October 2001.

Krypton Mission Example: NSSK for GEO COMM S/C

Can Krypton Propellant Satisfy Mission Needs?

Mission Parameters

- *Initial spacecraft mass*: **3760 kg**
- *Mission lifetime:* **15 years**
- *Thruster cant angle*: **40 deg.** (directional cosine loss)
- *Quantity of SPT-100 thrusters*: **2**
- *Delta-V required:* (51 m/s/year)×15 years = **765 m/s**

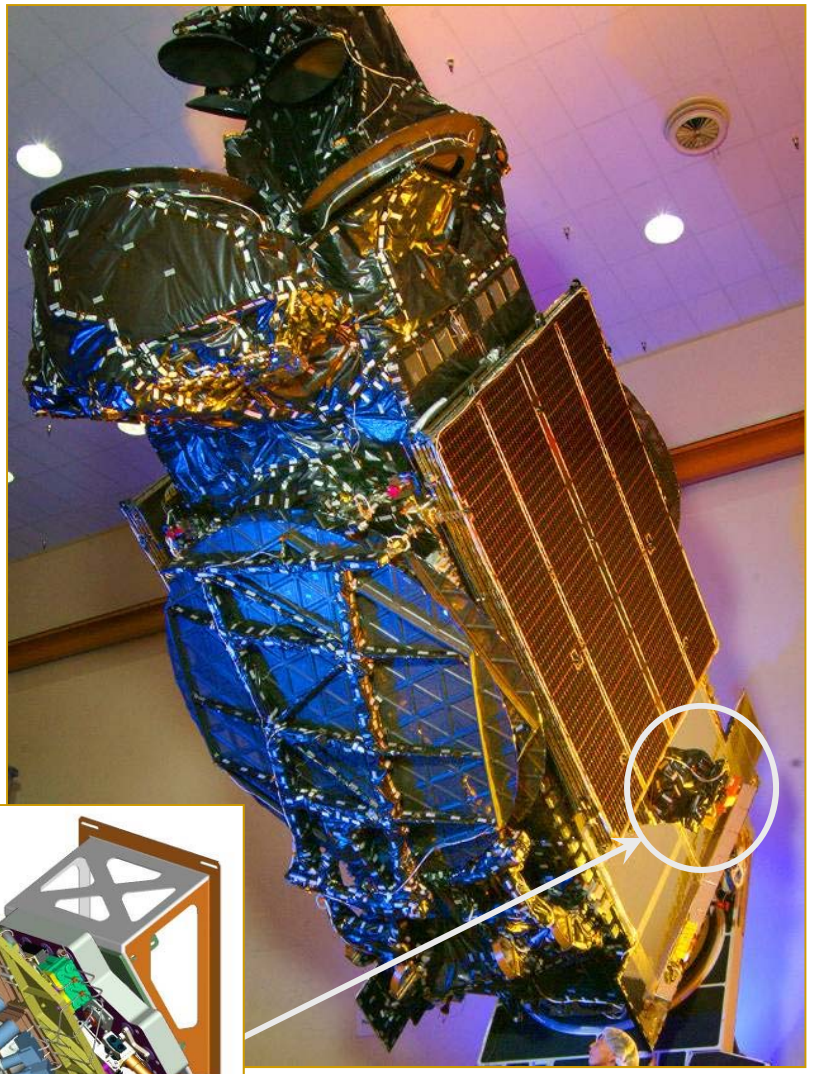

Geo Com. Mission Analysis for Kr

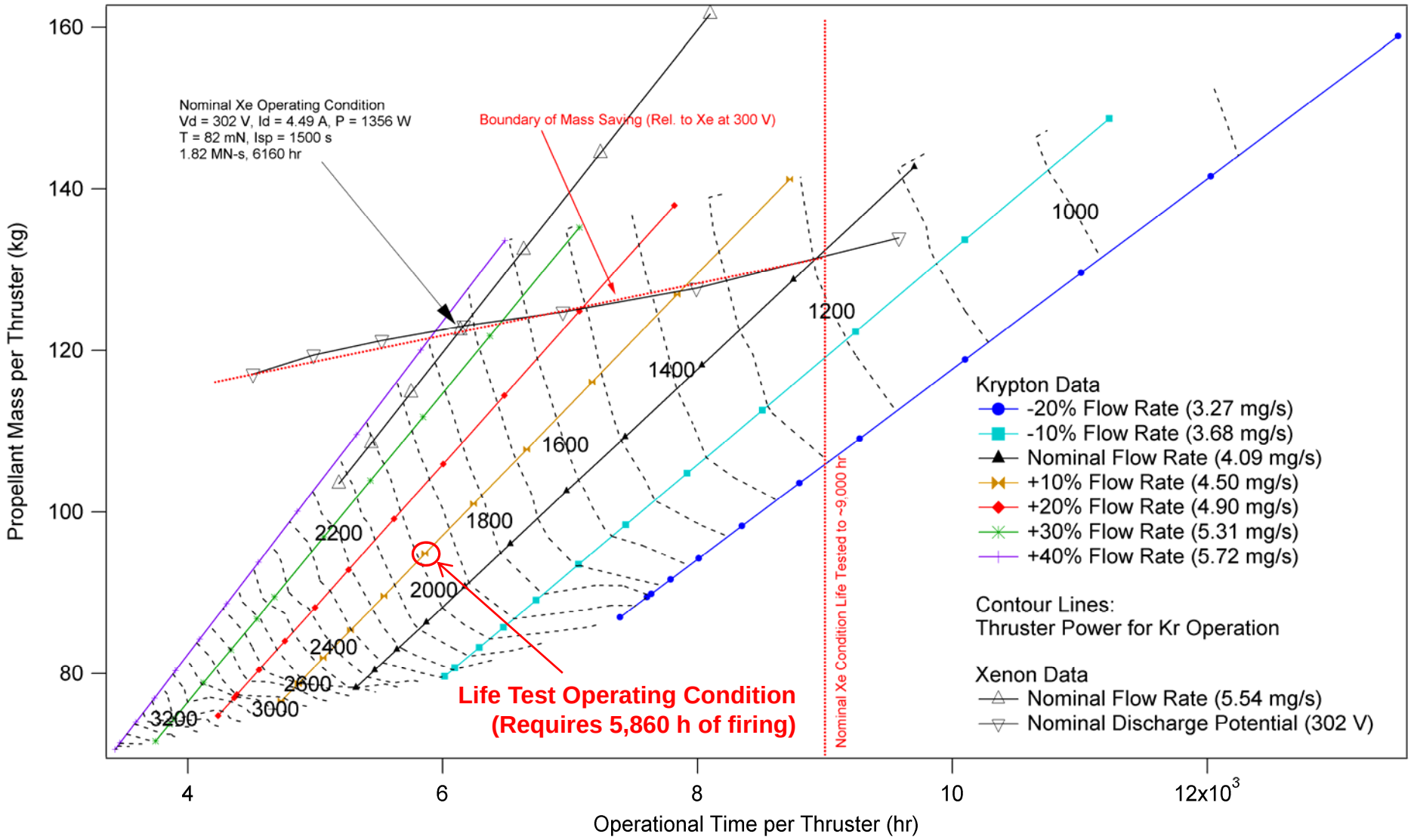

205 h Kr Life Test Overview

- **Performed in Chamber 1 at AFRL**
  - 2.4 m dia., 4.1 m length
  - Firing Pressure: 2.3×10^{-5} Torr
- **New flight model SPT fired**
  - Powered by laboratory power supplies
  - Propellant dispersed by digital mass flow controllers
  - Data acquisition system measured potentials and currents at 0.5 Hz
- **Insulator erosion measurements**
  - Performed with optical profilometer
  - After 0, 100, and 205 h of firing
- **Faraday probe sweeps**
  - Taken every 30 min. at r = 100 cm
  - Some missing time periods due to malfunctioning computer program

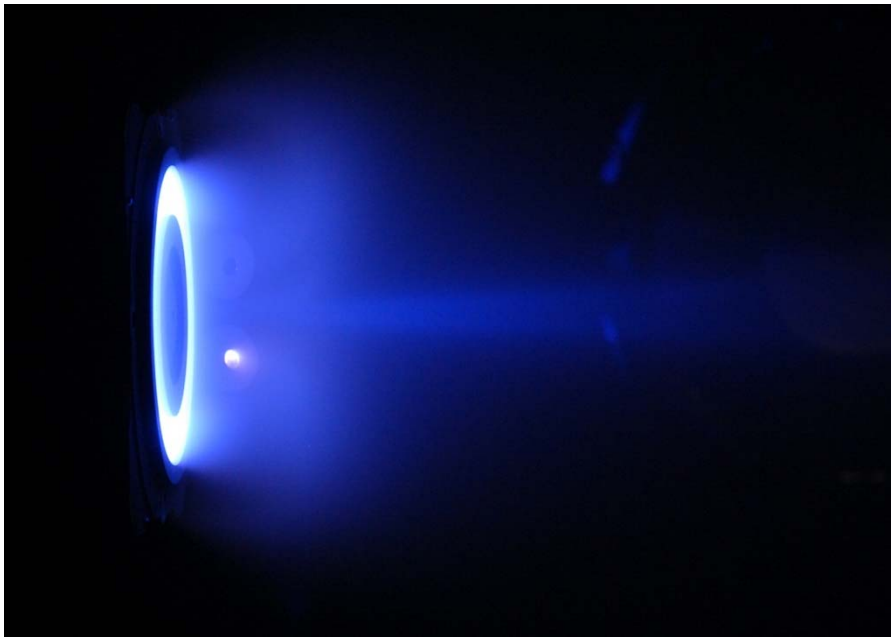

Life Test Operating Condition: 393 V, ma = 4.17 mg/s

	Performance Testing	Life Testing
m_a	4.17 mg/s	4.17 mg/s
m_c	0.32 mg/s	0.32 mg/s
V_d	393 V	393 V
I_d	5.03 A	5.14 A
P	1977 W	2022 W
T	86.7 mN	-
I_{sp}	1966 s	-
Total Eff.	0.423	-

Life Test Chronology

Date (2012)	Duration (h)	Cumulative Firing Time (h)
Sept. 7-10	74.35	74.35
Sept. 11-12	25.66	100.01
Sept. 18-19	31.37	131.37
Oct. 5-6	54.31	185.69
Oct. 8-9	19.33	205.01

Five separate firings totaling 205 hrs.

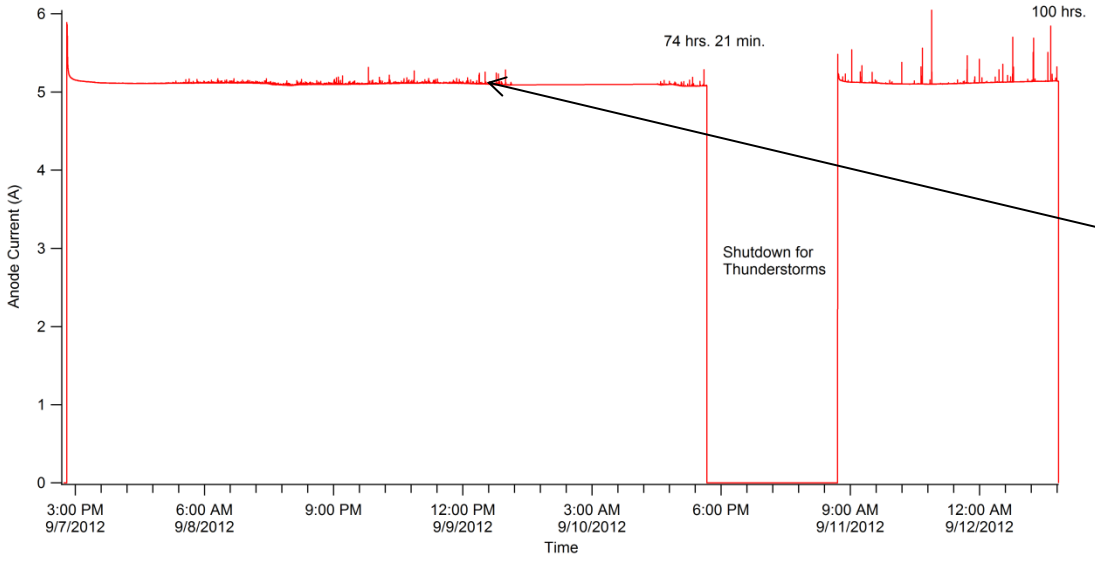

Anode Current, First 100 hours: Sept. 7-12

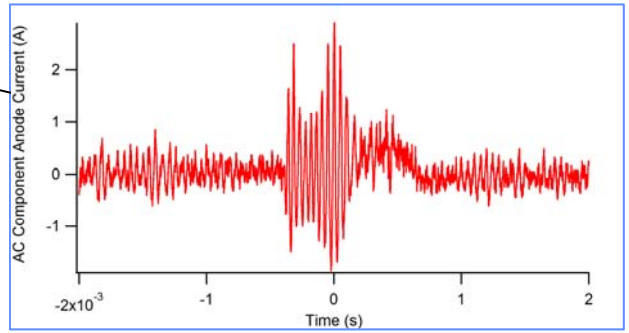

Current spikes from expelled graphite embers

Chamber Setup and Faraday Probe

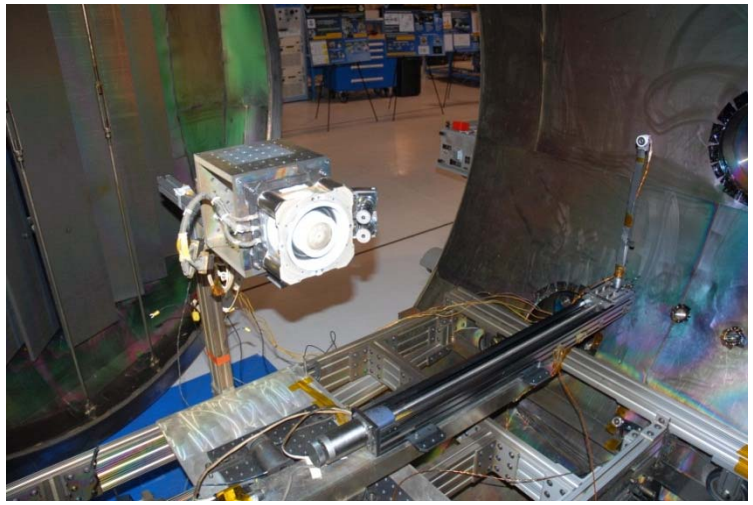

Faraday probe at r = 100 cm

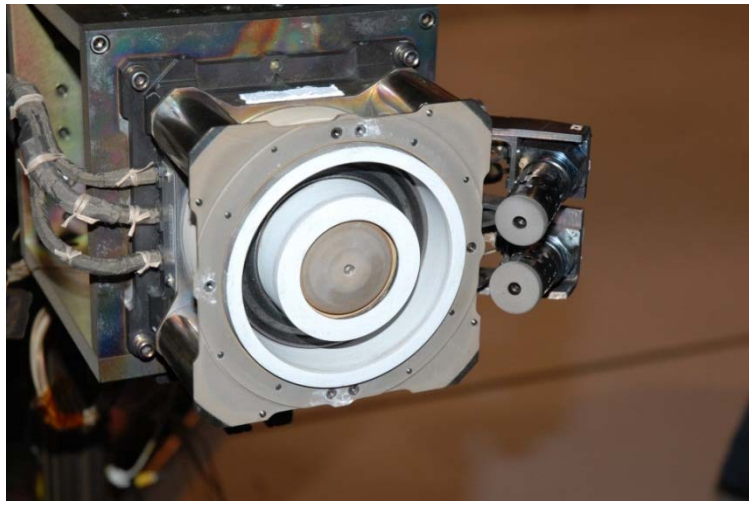

SPT-100 before firing

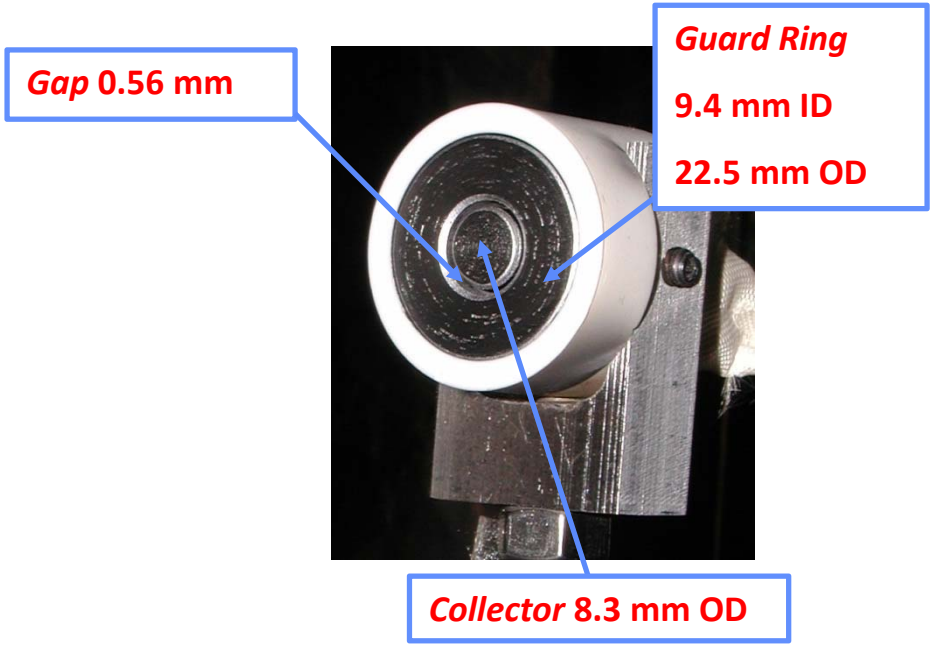

Probe dimensions

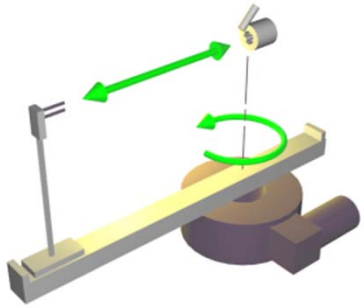

Probe motion system

Anode and Beam Current

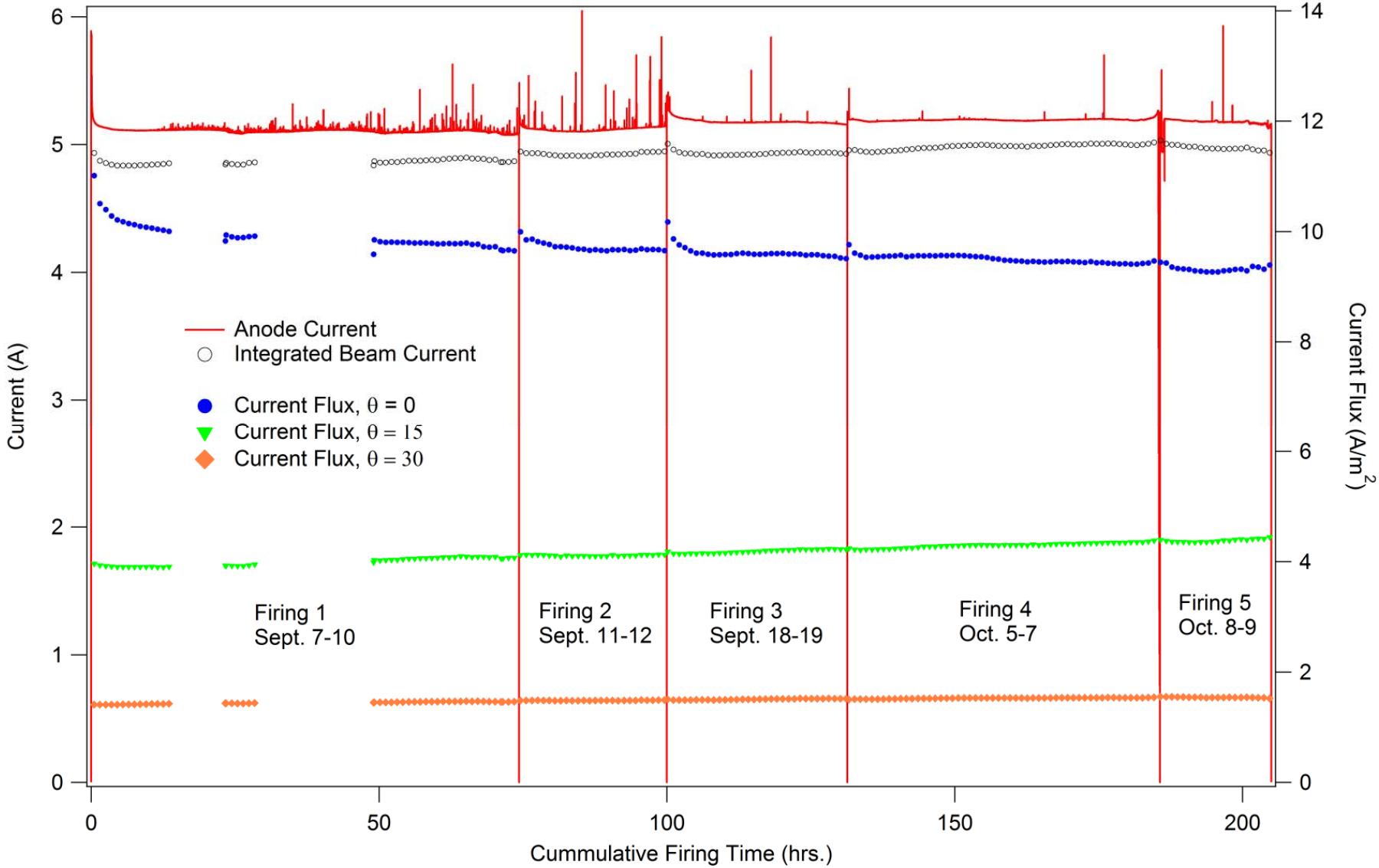

Faraday Probe Traces

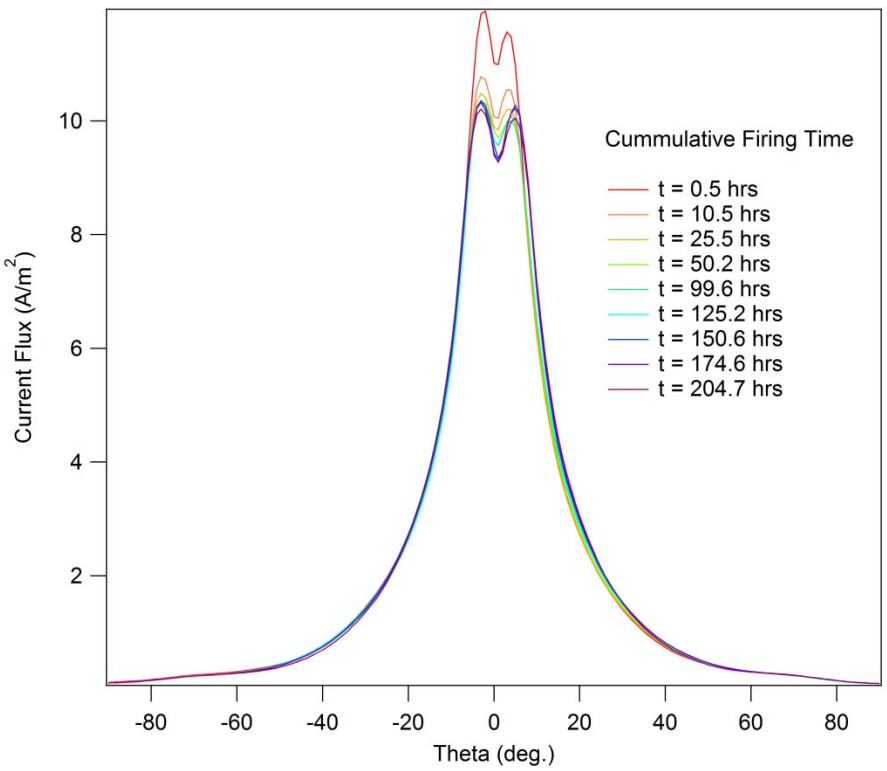

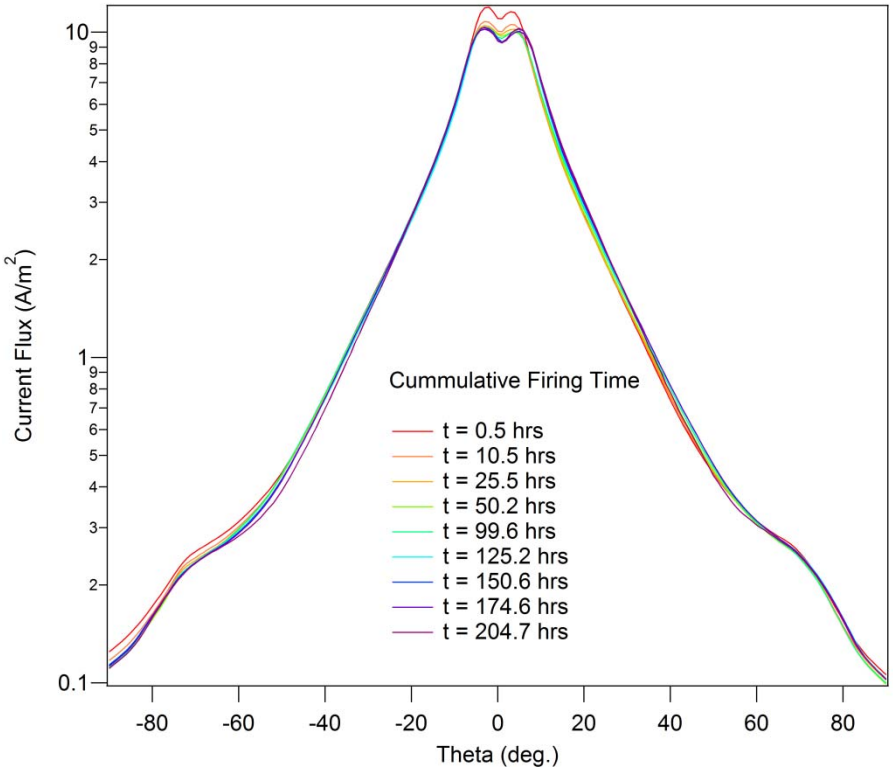

Faraday probe sweeps show consistent charge flux over the life test. (Measurements shortly after SPT ignition are slightly greater.)

Optical Profilometer

- **STIL CHR 150 confocal chromatic optical sensor**
  - Uses highly chromatically aberrated light to measure depth
  - Wave length of focused light on subject corresponds to depth
- **Motion control for scanning**
  - Stepper motor driven stages
  - X-Y motion using linear stages
  - Polar coordinates using rotation stage
- **24 mm depth of field optical pen**
  - Accuracy of 3.0 µm
  - Lateral resolution of 50.0 µm

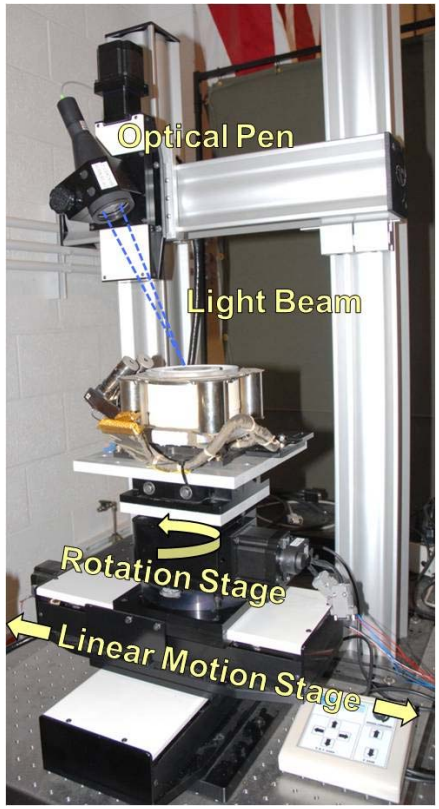

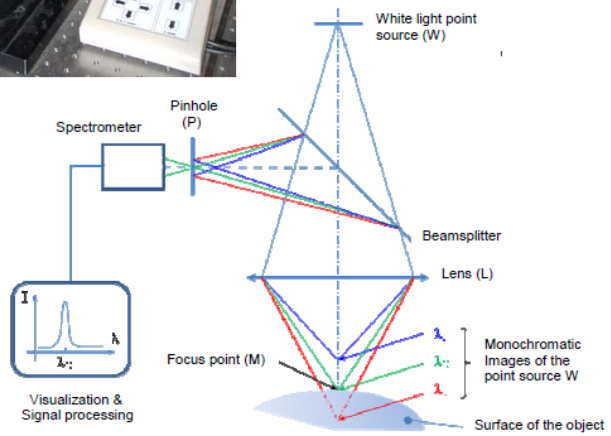

(Graphic from www.stilsa.com)

SPT-100 Profilometery Measurement Setup

- **Profiles taken in radial spoke pattern**
- **Polar coordinate step sizes**
  - *r*: 0.10 mm
  - ϕ: 2.5 deg
- **No averaging**
- **Scan duration: 50 hours**
- **Tilted pen:**
  - Allows optical access to channel interior
  - 24.1 deg. from vertical for SPT measurements
  - Data processing requires coordinate transformation

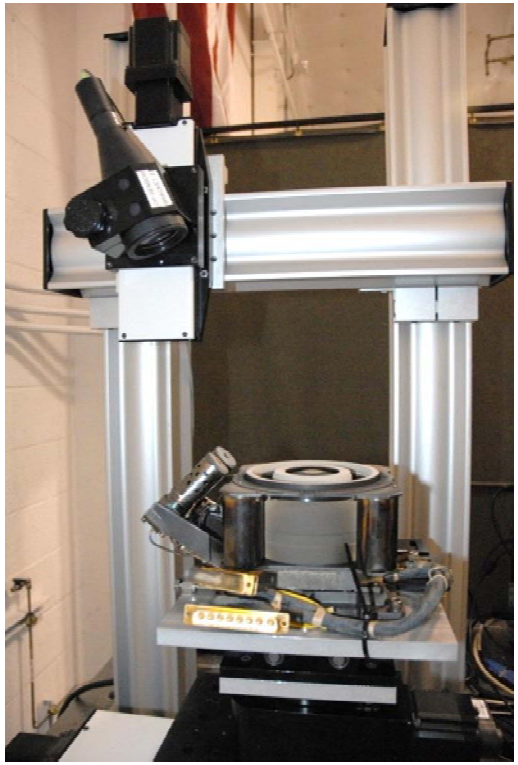

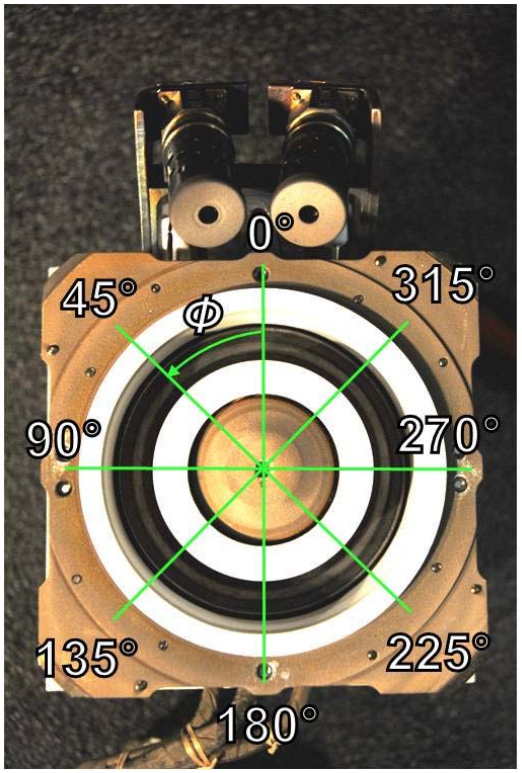

Insulator profile scans made in azimuth angle increments of 2.5 deg.

Visual Erosion Comparison

100 h (significant graphite deposits)

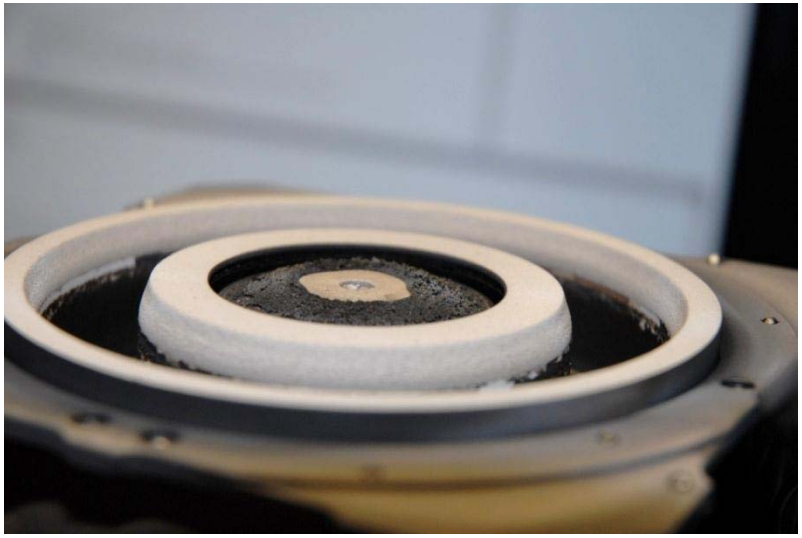

205 h (graphite deposits reduced)

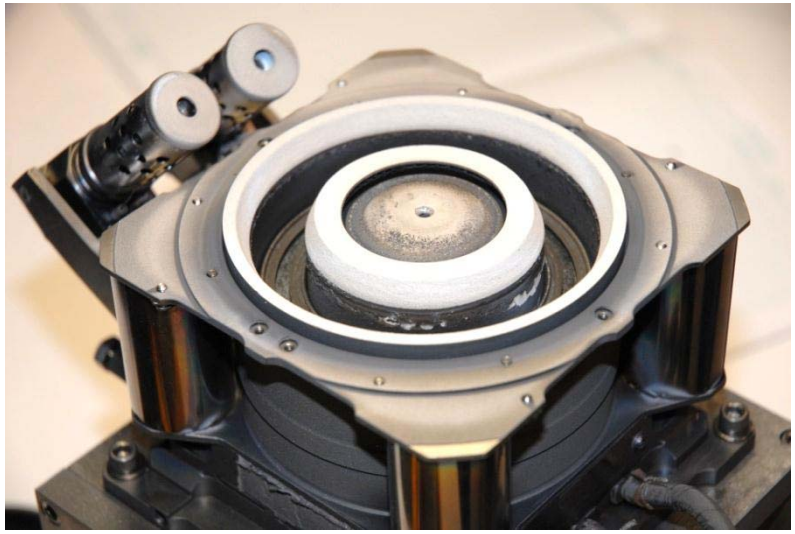

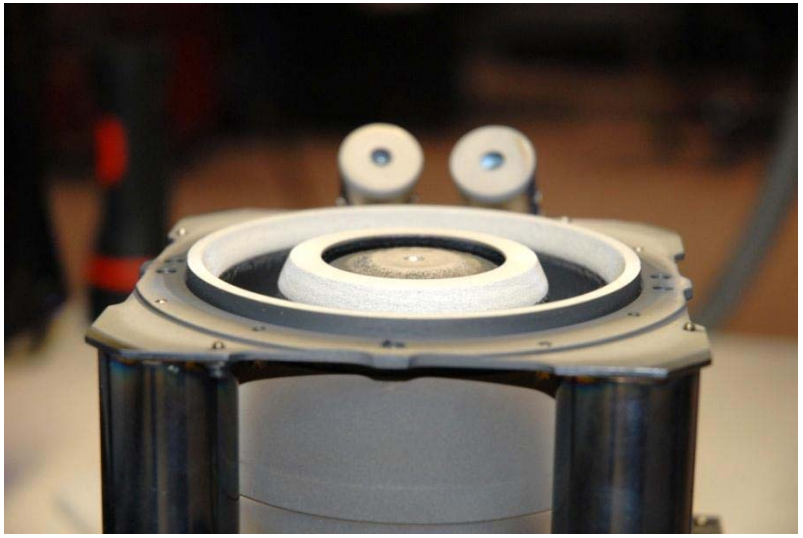

Profile Comparison

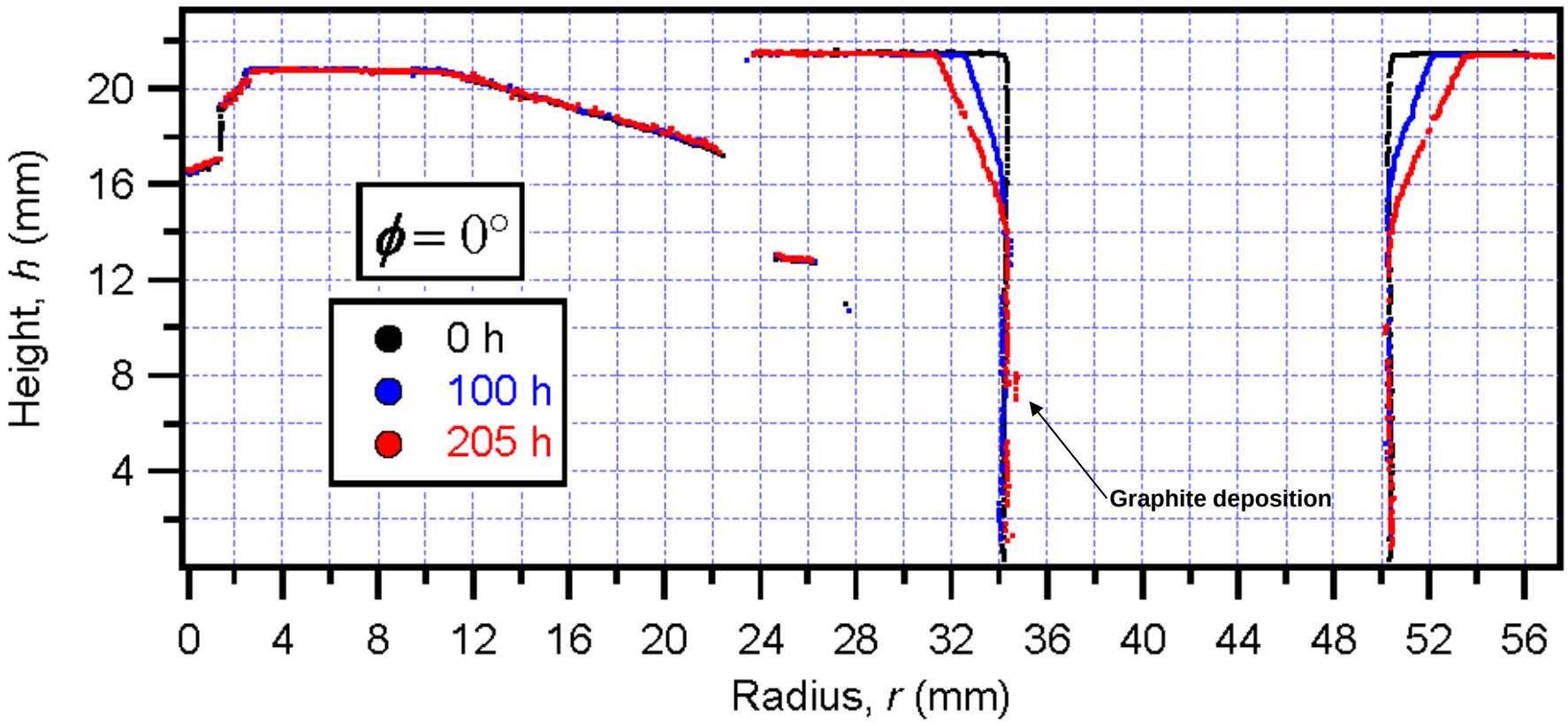

Erosion Calculation

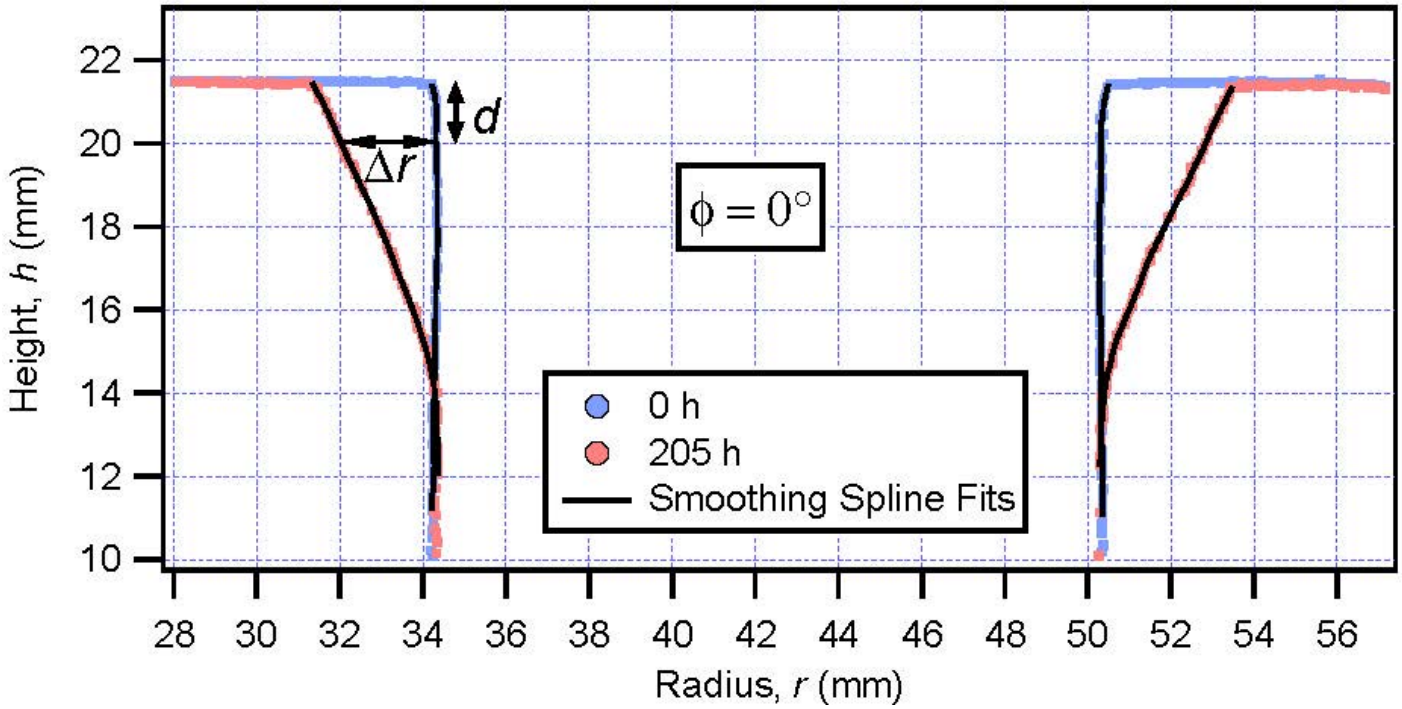

- Smoothing splines fit to channel walls for each data set
- Erosion, Δr, is calculated as the difference in radial coordinates between the smoothing spline curve fits as a function of channel depth measured from the exit plane.

Erosion Profiles

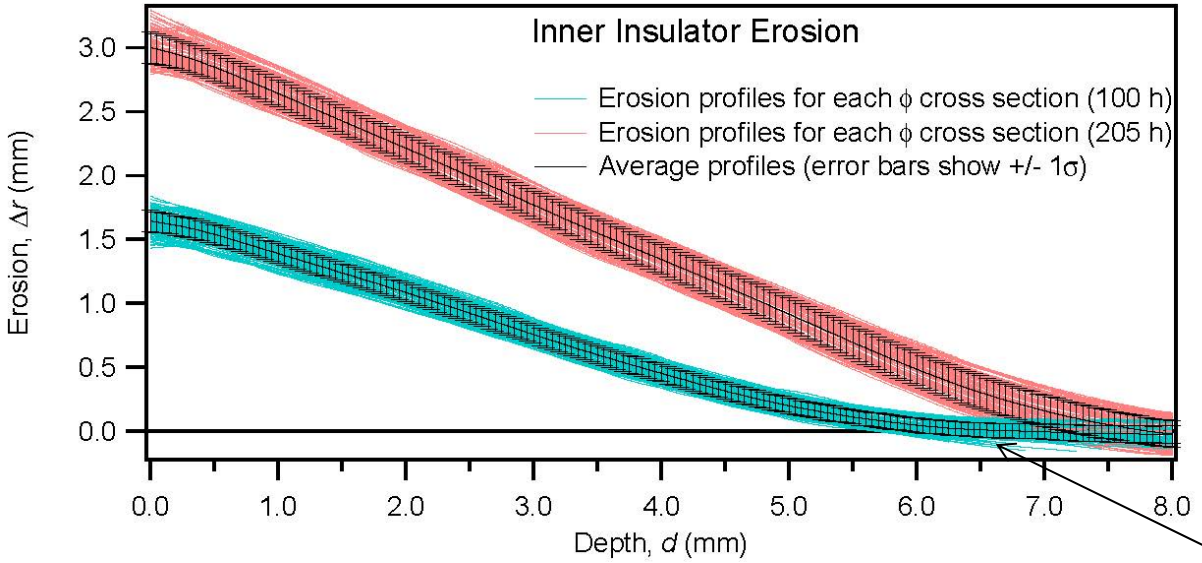

(Graphite deposition accounts for negative values.)

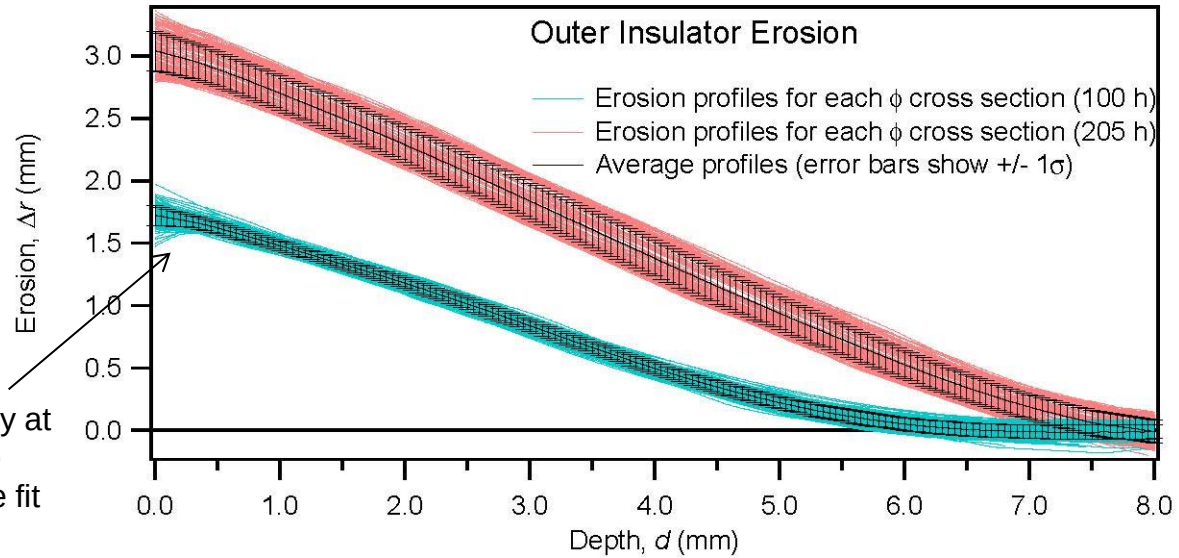

(More uncertainty at exit plane due to smoothing spline fit near corner.)

Mean Erosion Profile Comparison

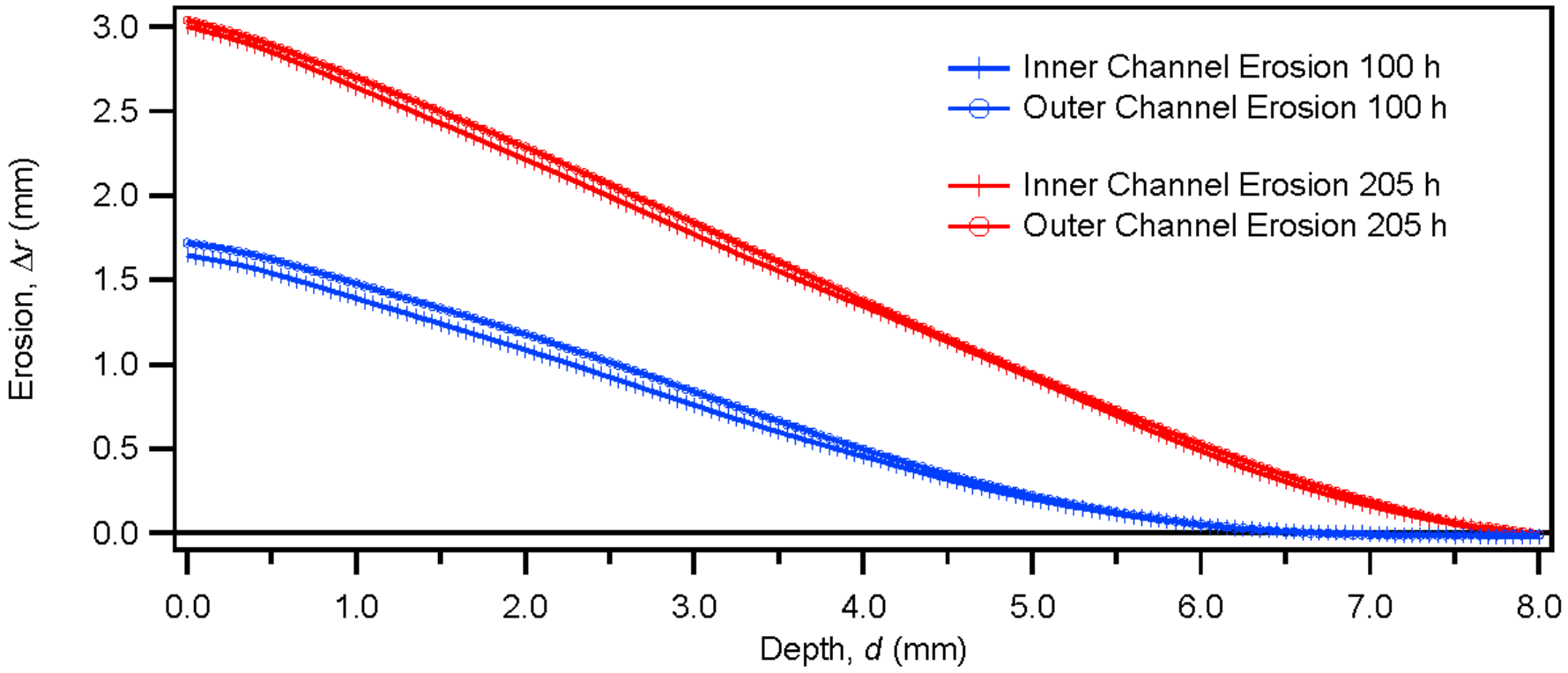

Erosion similar for inner and outer insulators

Erosion Rates

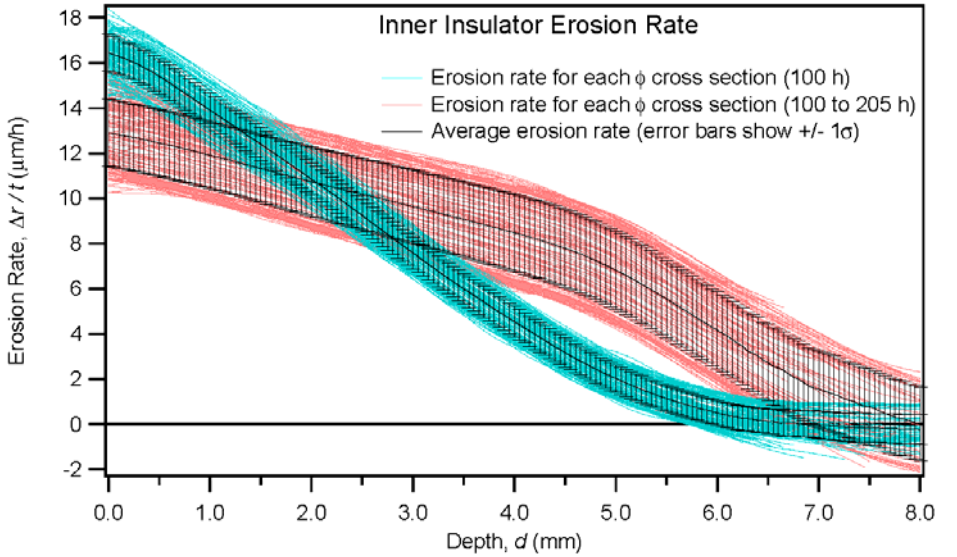

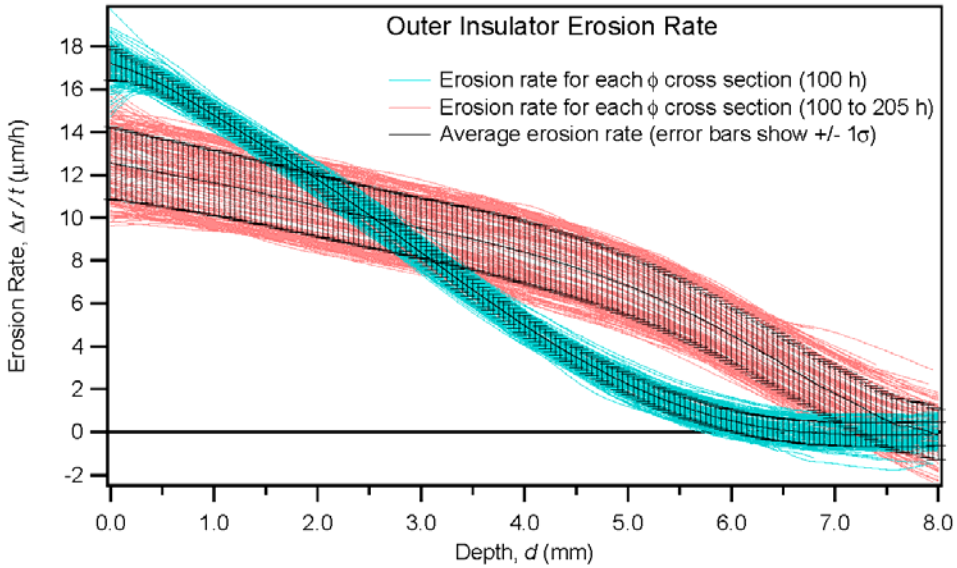

Mean Erosion Rate Comparison

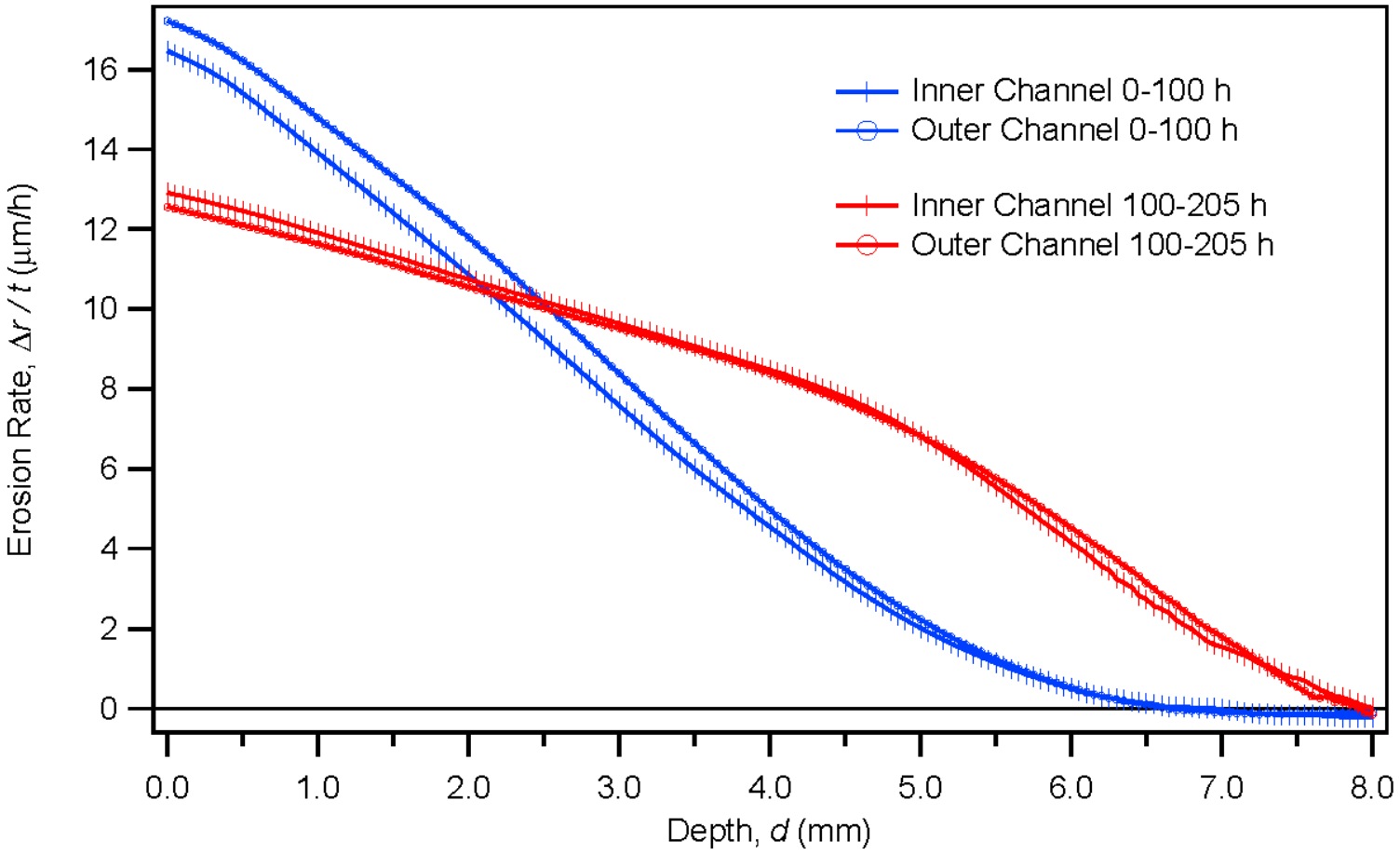

Azimuthal Characteristics of Erosion

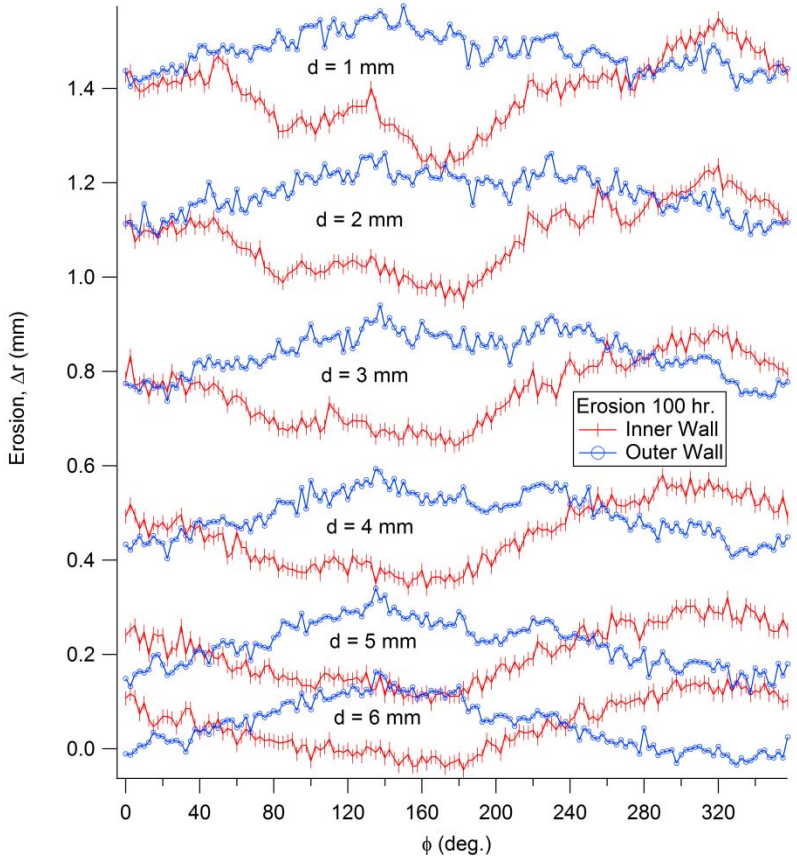

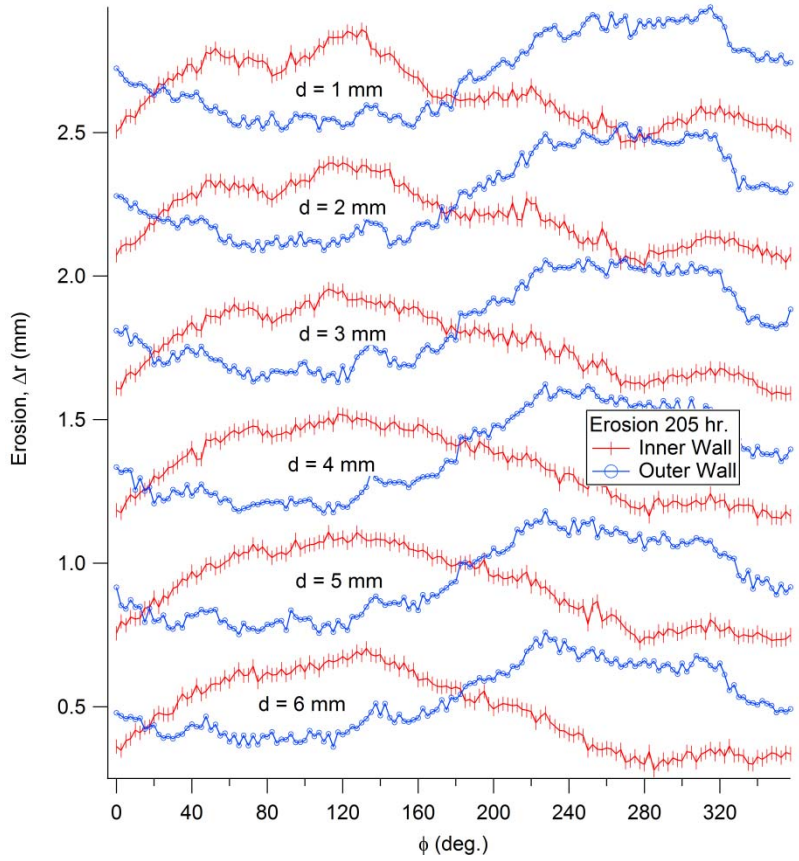

Variations are no larger than experimental uncertainties

- Periodic out-of-phase erosion between inner and outer insulator suggest a small discrepancy in the radial coordinates between data sets
- Sources of error: remounting thruster, hysteresis in stepper motor position, large radial step increment (0.10 mm), drift in optical pen zero between data sets, coordinate transformation and alignment in data processing

Comparison to Xe Data

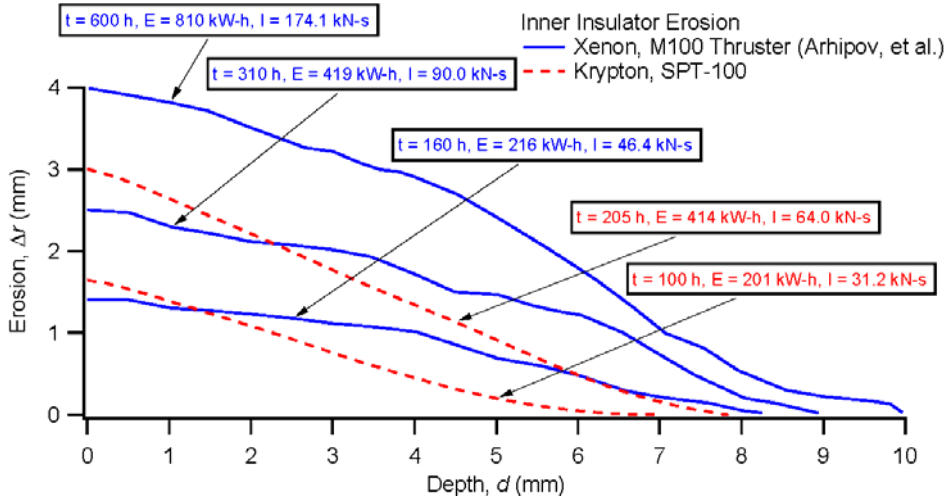

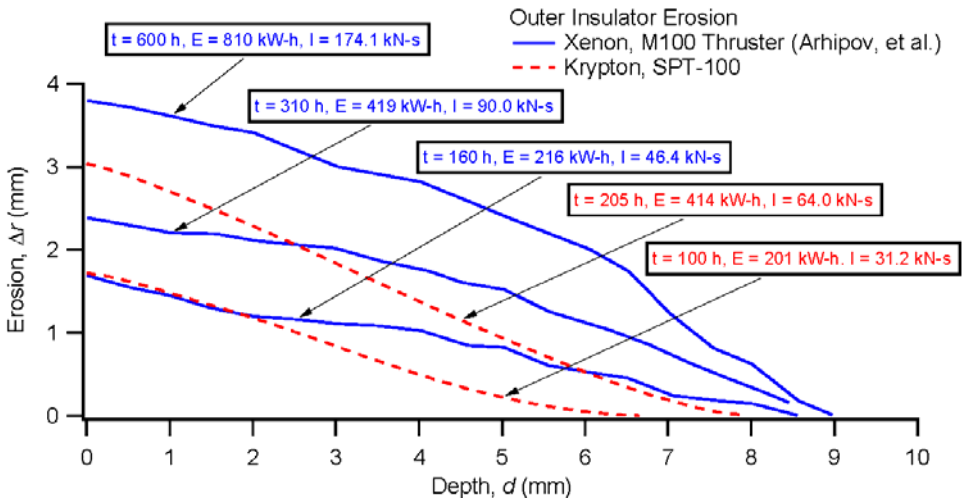

B.A. Arhipov, et al. "The Results of 7000-Hour SPT-100 Life Testing." International Electric Propulsion Conference, 1995. IEPC-95-39.

Conclusions

- Demonstrated ability of SPT-100 to operate at 50% higher than nominal power for an extended duration
- Obtained rare erosion data characterizing the early phases of boron nitride insulator erosion with Kr
- Kr erosion profile shows sputtering more concentrated at exit plane compared to Xe profile
- Example GEO COMM mission: Would SPT last 5,860 hours to complete mission? (Unclear from this short test)
  - Kr life test condition has the equivalent energy throughput of 8,800 hr of nominal Xe condition
  - SPT-100 is considered capable of firing 9,000 h at nominal condition
  - If correlation between erosion and energy throughput holds, SPT may be able to endure
- Long term life test would be required to validate Kr as an option for GEO COMM S/C propulsion
- Stronger radial magnetic field may lead to a more focused ion beam improving life time and performance

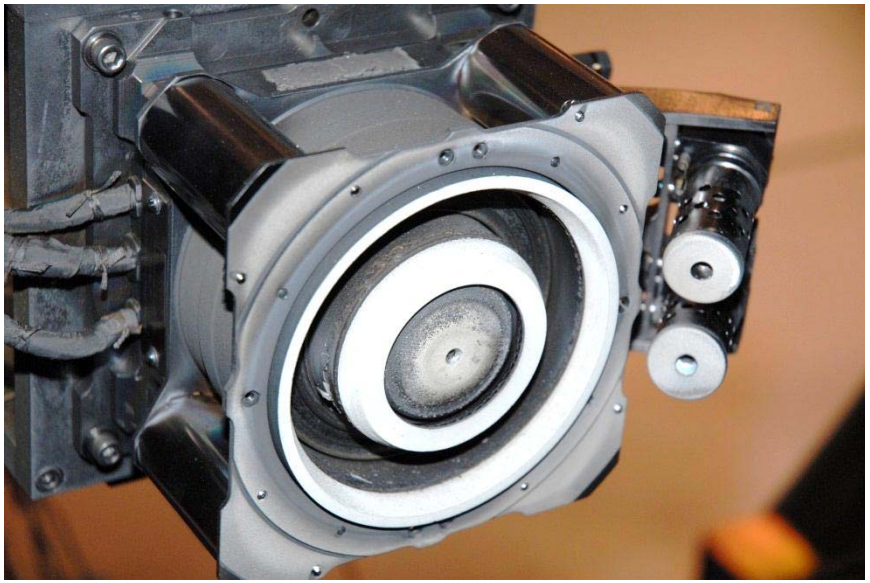

SPT S/N 29 after 205 hours of firing

Backup Slides

Optical Profilometer: Tilted Pen Geometry

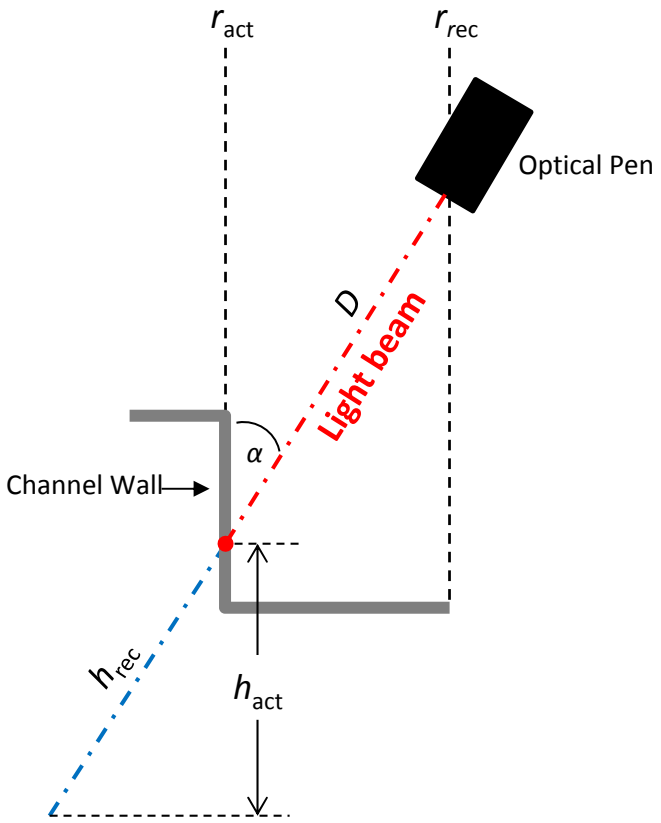

$$h_{max} = 24{,}000\ \mu m$$

$$z = h_{max} - h_{rec}$$

$$r_{act} = r_{rec} - h_{rec}\sin(\theta)$$

$$h_{act} = h_{rec}\cos(\theta)$$

Profilometer Data Processing

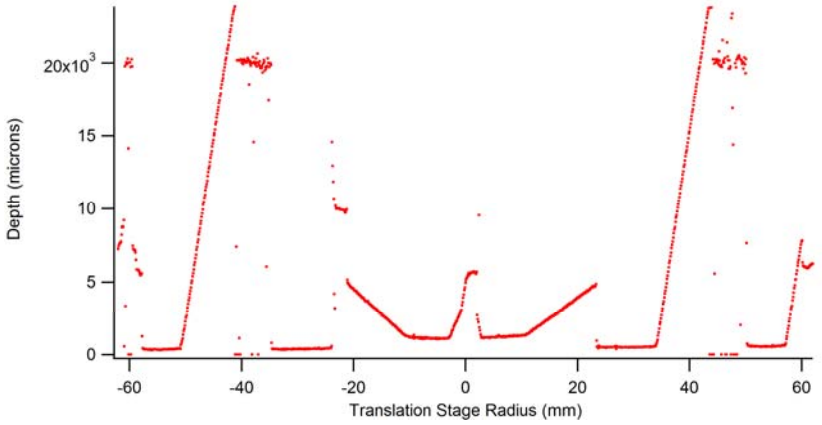

Raw data from profilometer slice

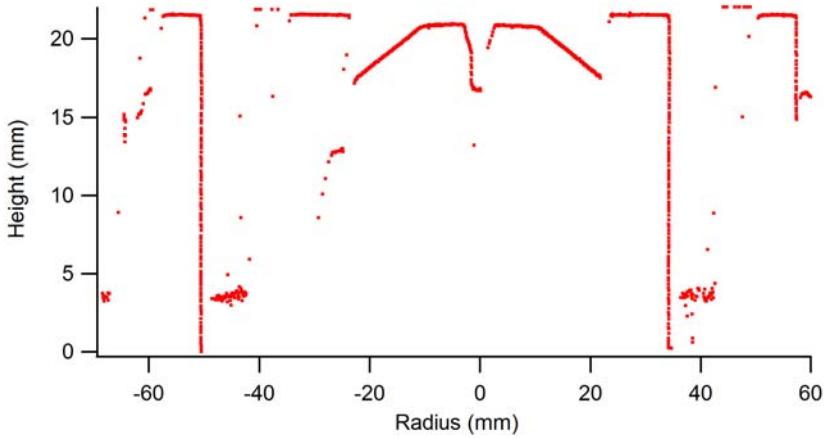

Coordinate Adjustments:

- **Coordinate transformation (from pen coordinates to rectilinear coordinates)**
- **Radius shift (to zero center of SPT at $r = 0$)**
- **Small rotation to correct for linear stage sag**

Profilometer Data Processing (cont.)

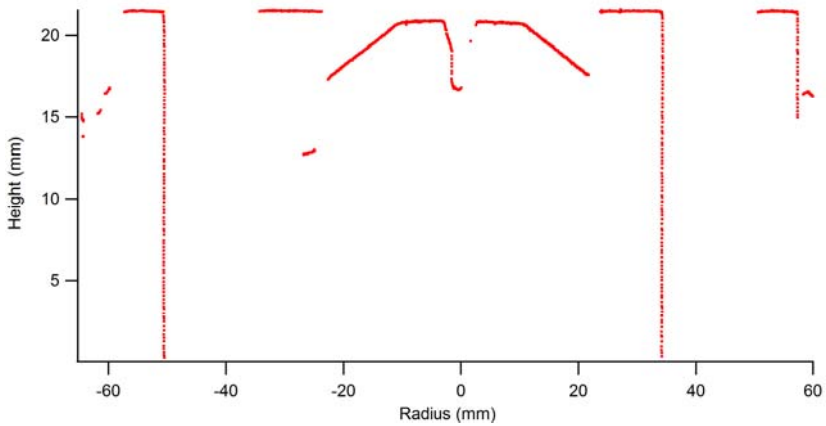

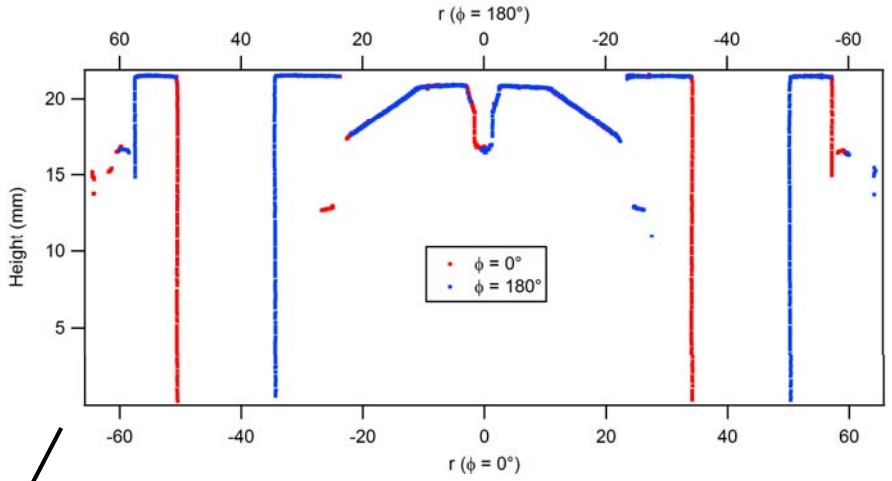

Filter data points based on signal intensity, channel location, and proximity to neighboring points

Combine profile from opposite (ϕ + 180 deg.) slice to form a complete channel profile for each ϕ measurement slice

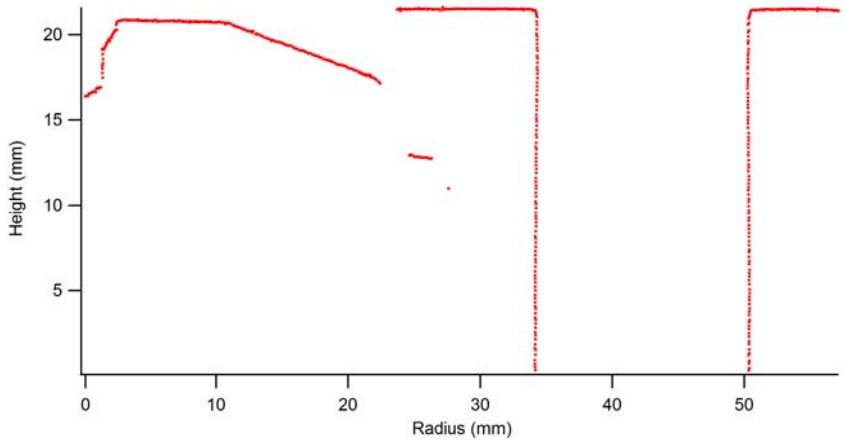

Fitting Channel Profiles

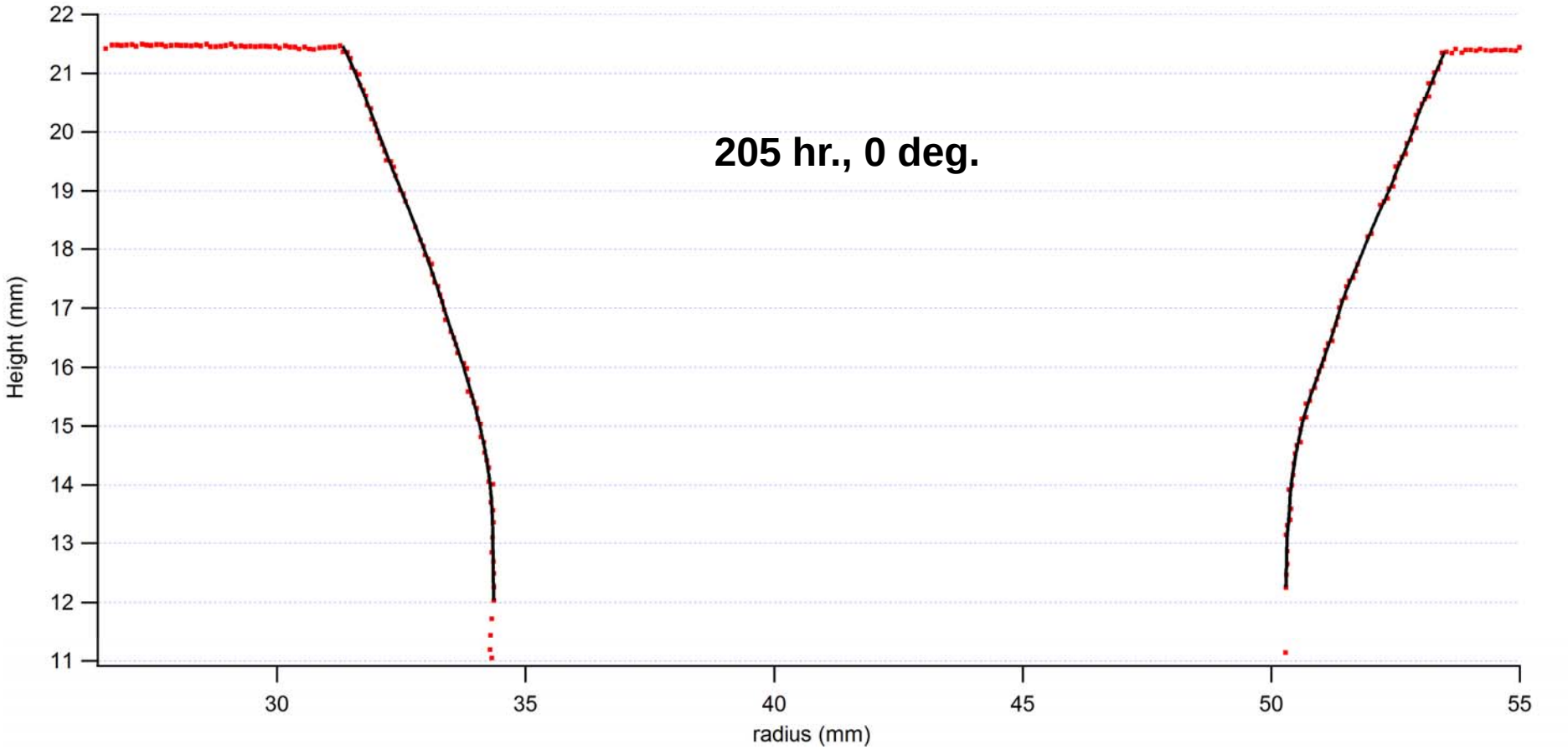

Fit smoothing splines to inner and outer channel walls at each ϕ location